Flood Mapping and Modeling on Fogera Flood Plain: A Case Study of Ribb River

School of Graduate Studies
Civil Engineering Department
Hydraulic Engineering Stream

By Zelalem Abera

Flood Mapping and Modeling on Fogera Flood Plain:
A Case Study on Ribb River

By
Zelalem Abera

A Thesis submitted to School of Graduate Studies, Addis Ababa Institute of Technology in partial fulfillment of the requirements for the degree of masters of Science in Hydraulic Engineering.

,

Ethiopia
June, 2011

CERTIFICATION

I, the undersigned, certify that I read and hereby recommend for the acceptance by the Addis Ababa University a dissertation entitled: ***Flood Mapping and Modeling on Fogera Flood Plain*** in partial fulfillment of a degree of Masters of Science in Hydraulic Engineering.

Dr. Ing. Dereje Hailu

(Supervisor)

Date: ----------------------------

**Flood Mapping and Modeling on Fogera Flood Plain:
A Case study of Ribb River**

Thesis Submitted to Addis Ababa Institute of Technology, School of Graduate Studies in partial fulfillment of the requirements for the Degree of Masters of Science in Civil Engineering with Hydraulic Engineering.

Date defended--------------------

Members of Examining Board

--	----------------------------
(Chairman)	(Signature)
--	-----------------------------
(Advisor)	(Signature)
--	-----------------------------
(Internal examiner)	(Signature)
---------------------------------------	-----------------------------
(External examiner)	(Signature)

Dedicated to my Mom-Atsede Weldemariam: You deserve even more.

Abstract

Flood occurs repeatedly in Ethiopia and cause tremendous losses in terms of property and life, particularly in the lowland areas. The majority of flood disasters' victims are poor people living in nearby stretch of floodplain. Therefore, the study was carried out to perform floodplain analysis and risk assessment of Fogera and nearby areas.

This research involves the integration of HEC-Hydrologic Modeling System (HEC-HMS) and HEC-River Analysis System (HEC-RAS) with Geographic Information Systems (GIS) to develop a regional model for floodplain determination and representation.

The study describes the flood extent and depth in the area for different flow conditions derived from the historical flow data of the Ribb River. The hydrologic model is calibrated using HEC-HMS for hourly time series data for return periods of 2, 10, 50 and 100 years. The value derived by the hourly data of the HEC-HMS is compared with different frequency analysis methods. One dimensional hydraulic model HEC-RAS with HEC-GeoRAS interface in co-ordination with ArcGIS was applied for the analysis.

Triangulated Irregular Network (TIN) was prepared from shape file generated from spot elevations of the floodplain through field survey data and the DEM of the study area in ArcGIS. Required data sets as stream centerline, banks, flow paths and cross sections were prepared in HEC-GeoRAS thus, creating import file and imported in HEC-RAS. In HEC-RAS, boundary condition for downstream were defined. Similarly, flood discharges for different return periods were also inputted and steady flow analysis was done for the results.

The result of hydrologic model by HEC-HMS shows a flow value of 91.8m^3/s, 202.4 m^3/s, 273.1m^3/s, and 308.4m^3/s for return periods of 2, 10, 50 and 100 respectively. The result was compared with the frequency analysis using event flow values of the Ribb River.

According to the food map, the flooded area for the return periods 2, 10, 50 and 100 years are 12.63km^2, 18.63km^2, 21.31km^2 and 22.5km^2 respectively. The classification of flood depth area showed most of the flooding area had water depth less than 1.5m. On the other hand 88% of agricultural land, 11.6% of agro-pastoral land and 1.36% River is inundated by the flood.

Key words: HEC-HMS, HEC-RAS, TIN, DEM, flood map

Acknowledgement

First and for most, I would like to thank my holy father, God and his mother, for his care, support and endless love during my stay in Addis Ababa University.

I am indebted to my respected Advisor, Dr. Dereje Hailu for his continuous guidance, advice and expedience from the proposal preparation to thesis finalization. His constructive comments, untiring help, guidance and practical suggestions inspired me to accomplish this work successfully. I would like to express my deepest gratitude to Dr. Semu Ayalew for his support in material and advise necessary for the work.

I remember Hailay Zeray for his friendly support in sharing knowledge which initiated me to continue the research in a safe way. His smiley and bright face make me see myself where I am. I express my special gratitude to Haileyesus Belay for his unrepayable idea, advice, suggestion and comments. I also offer my sincerest gratitude to him for his support financially during finalizing proposal.

My classmate friends, you are so friendly and you deserve my genuine appreciation. I enjoyed pleasant time with you. Thank you so much all of you.

Finally, I offer my greatest appreciation to my beloved mother, Atsede Weldemariam for her prayer.

Table of contents

List of Figures

List of Tables

List of Acronyms

amsl: Above Mean Sea Level

CN: Curve Number

CFCA: Canadian Foundation for Climatic and Atmospheric sciences

DEM: Digital Elevation Model

DTM: Digital Terrain Model

DMC: Double Mass Curve

EV: Extreme Value

FA: Frequency Analysis

HEC-RAS: Hydraulic Engineering Center for River Analysis System

HEC-HMS: Hydraulic Engineering Center for Hydrologic Modeling System

I_a: Initial Abstraction

I_m: Maximum Infiltration

LN: Log Normal

LP: Log Pearson

LU: Land Use

LIDAR: Light Detection and Ranging

MoWE: Ministry of Water and Energy

NMA: National Meteorological Agency

RF: Rain Fall

TIN: Triangular Irregular Network

UH: Unit Hydrograph

1. INTRODUCTION

1.1 Back ground

The need to study the cause and effect of flooding has begun since flooding has become a problem to society when people and their valuables become affected. Historically many solutions have been proposed to mitigate the effects of flooding but knowledge on the actual cause effect relation is lacking. With the advent of digital computers, much emphasis has been on simulating and modeling of flood events and related characteristics and such is the main concern of this paper. The challenge here is to develop a reliable flood model to simulate flood events for Ribb catchment.

Causes of flooding may be either natural or human induced. Natural causes may be high and long lasting precipitation or extreme events such as earth quick and tsunamis. Man induced causes include failure of dam or levee. Mitigating in flood effects requires information on the flooding characteristics and how such characteristics propagate. Such information can be obtained through hydraulic models that are able to simulate flood events, depths, levels, velocity and timing over a distributed model domain and over the time dimension. Hydraulics models have the ability to solve such problems. HEC-RAS/HEC-GeoRAS is among the powerful model and is able to model flooding characteristics given that sufficient input data of good quality is available.

Open water flood forecasts are typically based on a two-step process in which a hydrological model is first used to route the flood and determine expected flow hydrographs at the site of interest. The peak flow from this flood routing analysis is then typically input into a steady flow hydraulic model, such as the HEC-RAS model, to determine the corresponding flood levels that would be expected along river reaches extending through populated areas along the flood plain.

There are a number of difficulties associated with this methodology. First, the application of hydrological models represents an approximate solution, since empirical relationships are used to approximate momentum effects.

Consequently, considerable time and effort can be expended in calibrating these models with historical (observed) data, and they may not be valid when extrapolated to extreme events.
The second difficulty associated with this approach is that it requires a steady flow hydraulic analysis to convert the peak flow forecast into a water level. This analysis must either be done in advance for a number of potential flow scenarios, or be done on a real-time basis for the specific forecast of peak flow. The former approach may result in unnecessary effort while the latter approach has the potential to lead to errors under the pressure of forecasting a major flood.

In hydraulic flood modeling, availability of data in the required spatial and temporal resolution is vital. Topographic data is one of such data used as input in hydraulic flood modeling. Digital Elevation Model (DEM) and/or its derivative Triangular Irregular Network (TIN) is major source of topographic data for representing floodplain and river topography. However availability and quality of the geometric data of river cross sections is a major limitation. For such availability of basic data sources, a high resolution DEM is a prerequisite. Even though there is still a gap to find this high resolution DEM to represent the topography of the study area, the 30m DEM is selected to best represent. The DEM coupled with the limited survey data aids to have a greater accuracy for construction of river topography and other properties.

On the other hand the availability of hydrologic data which is the major input for the hydraulic modeling and the flood delineation is also vital. The Ribb catchment doesn't possess much on this respect. The availability of synoptic station at Bahirdar and Debretabor aided for the development of the precipitation gage to represent the area. The later station has still an incomplete data. This makes the hydrologic model somehow difficult. There is still a biased and inconsistency of data for most of the time. The same is true for the flow data. The flow value is derived from the rating curve of the gage record.

1.2 Statement of the problems

The rainy season in Ethiopia is concentrated in four months from June to September. Large scale flooding is rare and limited to the lowland areas where major rivers cross to neighboring countries. However, intense rainfall in the highlands causes flooding of settlements close to any stretch of river courses.

The lower part of the Ribb catchment is known as one of the flood prone areas by the annual flooding in the Fogera floodplain. In 2006, extreme flooding affected 43,140 and displaced 8730 peoples respectively in the region (UNOCHA, 2006).

Even though flooding is frequently observed in the Fogera floodplain, the flood management strategy has not gone beyond strengthening rescue and relief arrangements and other post flood measures which are totally devoid of any pre-flood management and planning strategy to minimize loss of life, property and environment.

Information regarding the flooding characteristics and its effect are essential for flood management bodies for decision making in flood management strategies such as construction of flood protection structures (engineering structures), to develop flood emergency plan and human settlement planning.

With the advancement of new technology on flood modeling such as the hydraulic modeling (HEC-RAS) and GIS these days, it is possible to model flood extent, depth, distribution etc. in the temporal and spatial dimensions. Past flood study in the area however ignores these applications.

Another major necessity to conduct this research work is frequent happening of floods in the area. As the region is known as crop productive area of the country, most of the crops may be suffered. Lack of flood resistant engineering structures is another case for the necessity of the research to conduct.

1.3 Research Objectives

The following main and specific objectives have been formulated in this thesis work:

General objectives

The main objective of this paper is to enhance flood modeling and forecasting approach based on the actual field data and GIS.

Specific objectives

The specific objectives are summarized as follows:

1) Calibration of HEC-HMS and HEC-RAS considering different criteria
2) Comparing model output using daily and hourly time series data and selecting best for the flood modeling.
3) Developing flood map for the River and flood plain for different flow conditions and delineation of the flood map of the study area
4) Selecting and identifying vulnerable area of the study area

1.4 Study Area

1.4.1 Location

Ribb catchment is one of the largest sub-catchment in Tana basin found in the eastern part of the Lake. The catchment is located between $10^0 43'$ and $11^0 53'$ N Latitude and $37^0 47'$ Longitude. It has an area extension of $1540km^2$. This catchment is drained by the Ribb River which originates from Guna Mountain and finally joins Lake Tana in the vicinity where the River causes flooding. The downstream part of the catchment is part of the wide flat floodplain (Fogera floodplain) with a total area of $490km^2$.

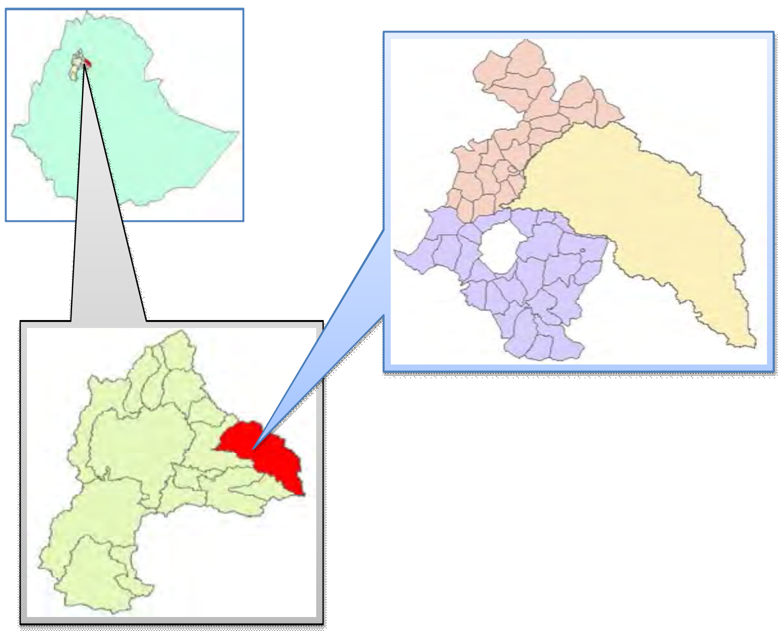

Figure 1: Study area map

1.4.2 Topography

The elevation of the catchment ranges from 1777 to 2150m amsl. The slope of the flood plain approximates 0.032% which is quite mild. The upstream of the catchment is highly mountainous while it is very flat at its lower reaches.

1.4.3 Land use and soil

Land use of the flood plain is mainly dominated by cultivated land. Most of the study area is characterized by cultivated lands as most of the area is rural.

The catchment is dominated by chromic luvisols and eutric leptosols. The two soil types cover almost 50% of the area. Eutric Fluvisols are another type of soils which dominated the catchment.

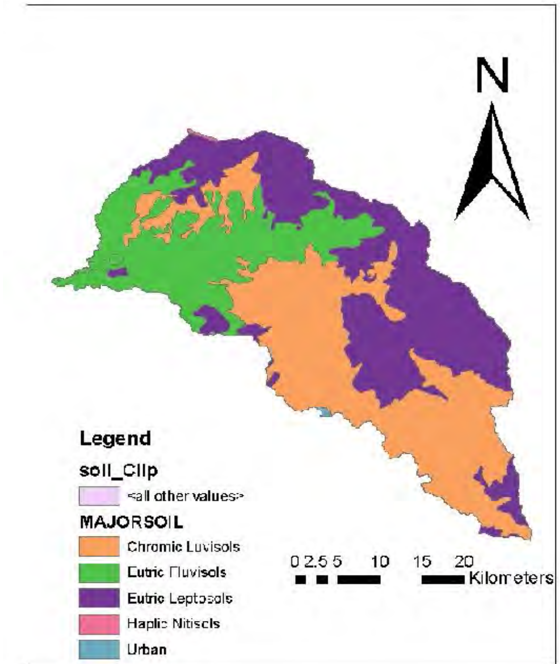

Figure 2: Soil type of the Ribb catchment

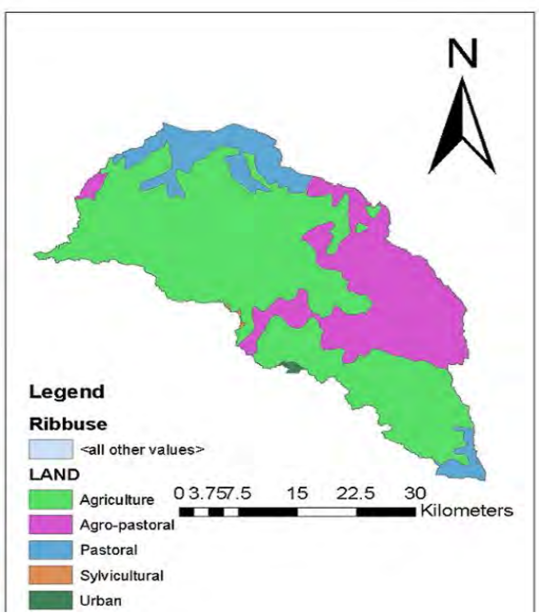

Figure 3: Land use of the Ribb catchment

1.4.4 Nature of the river channel

The Ribb River is formerly flowing what is now called old channel of the river. The new channel is made diverted at about 5km downstream of the bridge from the main road of the Gonder- Bahirdar highway. The separation of the two river channels is by the earthen embankment (dyke) for about 4-5km. while carrying out this research, the upstream of this junction has become very deep due to the extraction of the sand by the local farmers from the main channel for the dyke on the main channel. There may be little or no over flow from the new channel to the old. The only contribution of flow to the old channel is mostly local flows and very little overflow which is very difficult to quantify.

1.4.5 Rain fall distribution and flooding of the area

The catchment is characterized by a rainfall which amounts from 1100mm to 1500mm per year. These highest rainfalls were experienced during the months June, July, August and September. The rainfall distribution over the catchment is mono-modal; nearly 79% of the annual rainfall occurs from June to September. Peak flow in the River occurs in August with average monthly flow of $52m^3/s$.

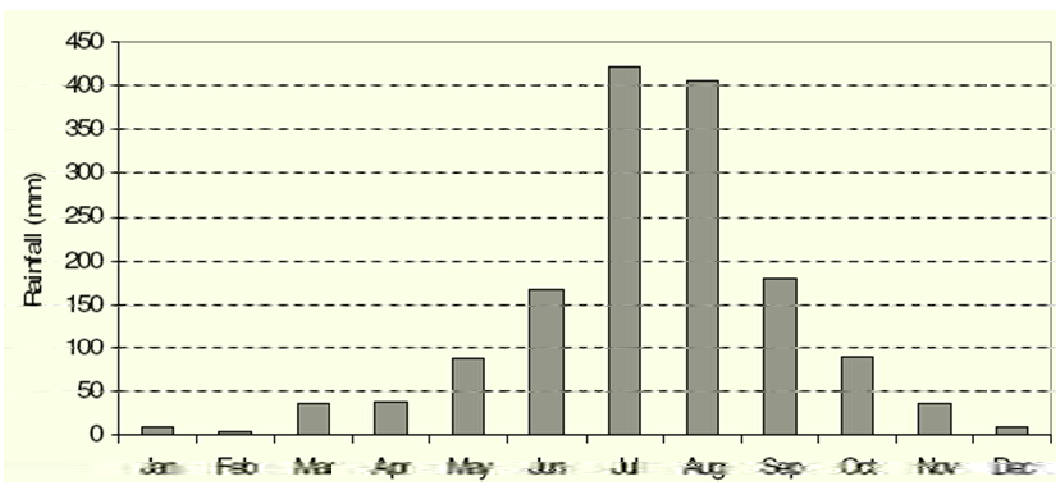

Figure 4: Mean monthly rainfall of the Ribb catchment

Flooding is the major problem in the downstream reach of the catchment. Severe flooding of the 1996, 1998, 1999, 2000, 2001, 2003 and 2006 are among the most events. The August 2006 flooding in the catchment was known for its long flood duration and devastation. Many people are forced to evacuate to other kebele for more than two months.

2. LITERATURE REVIEW

2.1. Hydrologic and Hydraulic Flood Modeling

Flood model is one of the means to understand the behavior of flood in a particular area. Model simulation can provide flood depth and extent. With the increase availability of the computing resources and the development of new models, flood hazard maps can be prepared at a high resolution with better accuracy for preparedness planning. Flood vulnerability map can be also prepared by integrating infrastructure and population data with the flood hazard maps. Flood models are the representation of hydraulic and hydrologic processes in the river channel and flood plain. Accurate representation of the actual processes is of paramount significance in predicting flood extent and depth, especially explaining the transient characteristics of river water flow in the model domain. Determining the variation of flow characteristics in the spatial and temporal resolution enables to design flood evacuation plan quite efficiently (Haile and Rientjes, 2005).

Physically based flood inundation model approaches solve the St. Venant equation using one dimensional (1-D) or two dimensional (2-D) numerical schemes. 1D model assumes change of stage, velocity and discharge along the longitudinal direction. These models are competent with hydrometric observations. In this model cross sections are taken at certain locations along stream wise direction and the geometry is assumed to be constant between the cross sections. Hydraulic energy, pressure forces, flow depth and velocity are assumed constant in the transverse direction and locations of the section may predetermine flow direction and condition.

2.2. Model selection

Selecting the best and appropriate model is an essential part in any research work. There are various criteria for choosing the most suitable model. According to Cunderlik and Simonovic (2003), the choice depends mainly on the requirement and needs of the research or project under interest. Cunderlik and Simonovic put the following as criteria:

a) Required output of the model
b) Availability of input data
c) Prices and availability of the model
d) The model structure

There are different flood modeling tools which have their own distinct model structure and solution procedures. Most widely used 1D flood modeling tools are; HEC-RAS, FLDWAV, ISIS, FLUCOMP, and MIKE11. Although today's researches prefer 1D2D interaction flood Models, the use of one dimensional flood model has also great significance in the research areas (Dhondia and Stelling, 2002). In this research the 1D hydraulic model with ArcGIS is used. The model has the capacity to simulate plain areas with high accuracy.

The models selected for this research are discussed as follows:

2.3. Hydrologic model (HEC-HMS)

Each HEC-HMS project requires three model data components: Basin Model, Precipitation Model and Control Specifications.

a) Basin Model

The basin model contains data, which represents the physical system of the study area in consideration. The descriptive data is entered by the user or imported from GIS and can be edited. Such data includes specification of the hydrologic elements of which the basin model is comprised, information on how the hydrologic elements are connected, and values of parameters for the hydrologic elements.

The capability to configure a basin model by "dragging-and-dropping" icons on a schematic display is provided. The element data can be edited with single element or global editors.

A basin model consists of hydrologic elements, of which there are seven types: sub basin, routing reach, junction, reservoir, diversion, source, and sink. The development of a basin model requires the specification of such elements and data that controls their 'behavior'.

The rib catchment has three sub-basins with the gauge located near Addis Zemen. The basin map is extracted from the GIS with the coordinate of the gauging station. The sub-basins are also provided with one reach each and a common point junction.

The Basin Model uses the following spatial data:

- ❖ River Reach Files for Stream network with junctions and diversions.
- ❖ Stream parameters (Muskingum K and X)
- ❖ Sub-basin data components: Loss parameters, routing parameters, and base flow values and computation methods.
- ❖ Downstream points

b) Precipitation Model

The Precipitation Model is a set of information required to define historical or hypothetical precipitation to be used in conjunction with a basin model.

Several options exist for specifying historical precipitation: (1) utilize cell based precipitation as required for the Modified Clark method; (2) import previously determined spatially-averaged precipitation; (3) Specify gages and their locations and weights and locations of index nodes, to be used in an automated inverse distance-weighting; (4) Specify gages and associated weights (e.g., from Thiessen polygons).

Even though the HEC-HMS can use any time step time series data, the case for flood modeling is effective with hourly data. The Fogera area rain gauge stations are not provided with hourly measurements except Bahirdar and Gonder posses synoptic measurements which have few data sets.

c) Control Specifications

Lastly, the Control Specifications define time-related information for a simulation, including the starting and ending dates and the time interval for computations.

The function of control specifications is to set the starting and ending dates and times and time (computation) interval. The time step for HEC-HMS model calibration for the catchment is divided into different time steps as for calibration, simulation and verification.

2.4. Hydraulic model Data (HEC-RAS)

The floodplain visualization was carried out using one-dimensional numerical model HEC-RAS. HEC-GeoRAS, an Arc GIS extension, is used as the interface between HEC-RAS and GIS for pre-processing and post-processing of the data in GIS. The availability of floodplain survey data for the new and the old alignment of the river, the pre and post processing using the HEC-GeoRAS is not complicated.

The geometric data of the flood plain and River is obtained from the digital elevation model (DEM) for the points where the plain showing less number of cross-sections. Water surface profiles, along the river reach under study, for floods of various return periods were computed with sub critical flow simulation. These profiles were exported to GIS and water surface Triangular Irregular Network (TIN) was generated. An intersection of the terrain TIN and water surface TIN results in flood map.

HEC-RAS Parameters

HEC-RAS uses a number of input parameters for hydraulic analysis of the stream channel geometry and water flow. These parameters are used to establish a series of cross-sections along the stream.

In each cross-section, the locations of the stream banks are identified and used to divide into segments of left floodway (overbank), main channel, and right floodway. HEC-RAS subdivides the cross sections in this manner, because of differences in hydraulic parameters. For example, the wetted perimeter in the floodway is much higher than in the main channel. Thus, friction forces between the water and channel bed have a greater influence in flow resistance in the floodway, leading to lower values of the Manning coefficient.

As a result, the flow velocity and conveyance are substantially higher in the main channel than in the floodway showing higher values of manning's resistance coefficient.

At each cross-section, HEC-RAS uses several input parameters to describe shape, elevation, and relative location along the stream:

- River station (cross-section) number
- Lateral and elevation coordinates for each (dry, un flooded) terrain point
- Left and right bank station locations
- Reach lengths between the left floodway, stream centerline, and right floodway of adjacent cross-sections (The three reach lengths represent the average flow path through each segment of the cross-section pair. As such, the three reach lengths between adjacent cross-sections may differ in magnitude due to bends in the stream.)
- Manning's roughness coefficients (may vary horizontally or vertically)
- Channel contraction and expansion coefficients
- Geometric description of any hydraulic structures, such as bridges, culverts, and weirs

Data requirements for the HEC-RAS model:

a) **Geometry Data**

Cross section data represent the geometric boundary of the stream. Cross sections are located at relatively short intervals along the stream to characterize the flow carrying capacity of the stream and its adjacent floodplain. Even though it is not a must, it is advisable to take cross section at constant interval.

Cross sections are required at representative locations throughout the stream and at locations where changes occur in discharge, slope, shape, roughness; at locations where levees begin and end; and at hydraulic structures (bridges, culverts, and weirs).

The required information for a cross section consists of: the river, reach and river station identifiers; a description; X & Y coordinates (station and elevation points); downstream reach lengths; Manning's roughness coefficients; main channel bank stations; and contraction and expansion coefficients. Points which are used to represent cross section in any floodplain modeling are:

a) Flow Data

Once the geometric data is entered, the necessary flow data can be entered. Steady Flow Data consist of: the number of profiles to be computed; the flow data; and the river system boundary conditions. At least one flow must be entered for every reach within the system. Additionally, flow can be changed at any location within the river system. Flow values must be entered for all profiles.

Flow values can be imported directly from the HEC-HMS run for different hypothetical design storms or entered manually from the model run results. The flow data for the Rib River is assumed the one that is simulated by the HEC-HMS. Because of sedimentation and frequent washing of the River channel due to nature of the topography, the observed flow is assumed less.

b) Plan Data

Usually the first step in performing a simulation is to put together a Plan. The Plan defines which geometry and flow data are to be used, as well as provide a description and short identifier for the run. If the geometry and flow data do not exist, then this action is performed after their creation. Also included in the plan information are the selected flow regime and the simulation options.

2.5. ArcGIS

A GIS integrated with enterprise database management systems could manage large volumes of geospatial data to provide spatially distributed parameters for modeling However, use of GIS for modeling data management and integration is generally hampered by the differences in scale, precision, data structure, data meaning, representation of the reality, and others, between a GIS and a simulation model .

A hydraulic model, like any other model, is intended to be a realistic representation of the physical processes over time in a river channel or flood plain and gives decision makers an indication of the outcome for different options (Pullar & Springer, 2000).

The hydraulic model usually has the capacity to analyze, to predict and to solve engineering problems without taking into consideration the geographical prospective (McKiney & Cai, 2002). Under these circumstances, GIS becomes a valuable tool (Pullar & Springer, 2000) notes that there are strong grounds for believing that GIS has an important function to play because natural hazards are multi-dimensional phenomena which has a spatial component.

Many GIS integrated modeling applications have capitalized on using the GIS as a database manager and visualization tools. Data requirements, search method, governing algorithms, flood inundation extent and depth are the main area where these procedures might need to be modified and differ from the manual flood hazard map delineation processes (Norman et al., 2001). These enabling techniques which depend on the spatial capabilities of GIS, produce consistent modeling inputs as well as continual quality control (before, during and after the modeling process) where the benefits are nearly impossible to be obtained using the spreadsheets or other non-graphic methods of data organization. Moreover, once data is available in the GIS, they can be extracted, combined with other data, reformatted as needed for various modeling processes and even used to generate other inputs needed by the models.

Some of the common modeling issues that need to be tackled as described by Norman et al. (2001) are:

a) Data structure of the Digital Terrain Model (DTM)
b) Hydraulic model integration
c) Flood plain delineation
d) Accuracy of inundation maps

2.6. HEC-GeoRAS and the TIN

GeoRAS is an ArcGIS extension developed by the U.S. Army Corps of Engineers designed specifically to improve the data input process for HEC-RAS.

Operating within the ArcGIS environment, GeoRAS uses spatial data to develop, organize, and automatically enter input data into the HEC-RAS model.

The key data element that GeoRAS uses to develop the input data is terrain data, commonly referred to as a Triangular Irregular Network (TIN). One source for data used to develop TIN is a Digital Elevation Model (DEM).

DEMs exist in grid (raster cell) format which can be displayed within ArcGIS, if the proper extensions are installed. The quality of this data is based on its resolution, or cell size.

The smaller the cell is, the greater the resolution and accuracy. However, the smaller the cell size, the greater the memory and computation requirements. The usefulness of DEMs for developing terrain models should be determined based on the cell size and the level of hydraulic analysis to be performed. The more approximate the analysis is to be, the greater the cell size that may be used. This can best be represented by TIN of the study area.

The TIN model can be generated from the spot heights acquired from different sources in ArcGIS which included:

1) GPS surveyed data collected along the two river banks, with good accuracy.

2) The spot heights of the flood plains taken from the surveyed data which extend approximately far from both the left and right bank stations and cover the floodplain if topography permits.

3) River bed cross section elevation data accuracy.

2.7. Previous studies on Ribb catchment

Even though the Fogera area is characterized as high flooding prone area, there are still few studies applied. The current flood problem and lack of studies in the areas show the importance of the in-depth study.

Research conducted by Assefa et.al(2008) is centered on developing flood forecasting and early warning decision tools for the study area(Fogera flood plain) based on rainfall forecasts and hydrological model (HEC-HMS). It mainly focuses on a quantitative precipitation forecast based flood forecasting model using HEC-HMS rainfall runoff model for supporting flood early warning decision making.

Another study was conducted by the two researchers Gashaw and Legesse (2008) concentrates on flood mapping of hazard and risk in the area. They tried to show land cover change in the upstream (degradation) is contributing to flooding. Another most recent work was done by the River Side institution for the area and nearby pilot areas. They used 90m*90m DEM for topographical representation of floodplain and stream which has less accuracy resulting from larger cell sizes.

3. DATA COLLECTION AND ANALYSIS

3.1 Meteorological Data Availability and Processing

Before beginning any hydrological analysis it is important to make sure that data are homogenous, correct, sufficient, and complete with no missing values. Errors resulting from lack of appropriate data processing are serious because they lead to bias in the final answers, (Vedula, 2005). Generally, data should be appropriately adjusted for inconsistency, corrected for errors, extended for insufficient, and filled for missing using different techniques.

Basically a clear understanding of the hydro-meteorological conditions of the area is one of the basic requirements of any water resource management study. For this particular research work Meteorological, Hydrological, and Digital Elevation Model (DEM) data setting was undertaken for Ribb catchment and the corresponding floodplain area of Fogera.

Daily and some hourly rainfall and flow, maximum and minimum temperature data of different record length for some stations were collected from National Meteorological Agency (NMA) and Ministry of Water and Energy.

3.2 Estimating Missing Precipitation

A number of methods have been proposed for estimating missing precipitation. The station average method is the simplest one. The normal ratio and quadrant method provide a weighted mean, with the former biasing the weights on mean annual precipitation at each gauge and the later having weights that depend on the distance between gauges where recorded data are available and the point where the value is required. The isohyetal method is the fourth alternative.

Normal ratio method is used in this research paper. The method is used when the normal annual precipitation of the index stations differ by more than 10% of the missing stations. This is the case for the stations near the study area. The general formula for computing missing precipitation by this method is:

$$Px = \frac{Nx}{3}\left[\frac{P1}{N1} + \frac{P2}{N2} + \frac{P3}{N3}\right]$$

Where P_x = is the precipitation for the station with missing records

P1, P2 and P3 are the adjacent stations′ precipitation values

N1, N2, N3 are the long-term mean annual precipitation values at the respective stations and ‘**3**’ is the number of stations surrounding the station X.

3.3 Consistency and Homogeneity

Estimating missing precipitation is one problem that hydrologists need to address. A second problem occurs when the catchment rainfall at rain gages is inconsistent over a period of time and adjustment of the measured data is necessary to provide a consistent record. A consistent record is one where the characteristics of the record have not changed with time. Inconsistency may result from: change in gauge location, exposure, instrumentation, or an observational procedure is not real and on time.

To overcome the problem in consistency a technique most widely applied called double mass curve is used. Double-Mass Curve (DMC) analysis is a graphical method for identifying or adjusting inconsistencies in a station record by comparing its time trend with those of other stations nearby (Shaw, 1988).

Here accumulated annual values at the station in question are plotted against those of nearby reliable station or group of stations. An abrupt deviation in the slope of the Double-Mass Curve plot suggest some change not related to climatic variables, and adjustment should be made to the data on the basis of the ratio of the slopes of the two segments.

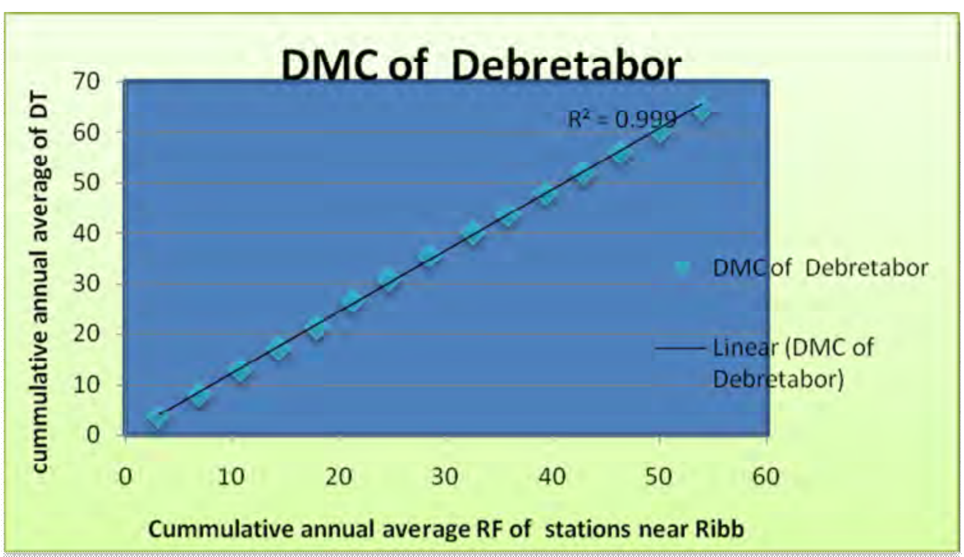

Figure 5: DMC of the Debretabor station showing high data consistency

3.4 Areal Precipitation

For analyses involving areas larger than a few square miles, it may be necessary to make estimates of average rainfall depths over sub watershed areas since a rain gauge records rainfall at a geographical point.

There are many methods available to determine the areal rainfall over the catchments from the rain gauge measurement: Arithmetic Mean, Thiessen Polygon, Isohyetal, Grid Point, Percent Normal, Hypsometric, etc. are available for estimating average precipitation over a drainage basin, (Shaw, 1988). Choice of methods requires judgment in consideration of quality and nature of the data, and the importance, use, and required precision of the result.

A Thiessen polygon method is most widely used method compared to others and is used in this research paper. In this method, weights are given to all the measuring gauges on the basis of their areal coverage of the watershed, thus eliminating the discrepancies in their spacing over the basins. All the stations in and around the basins are considered and a linear variation in the precipitation between two gauge stations is assumed.

.

In this procedure, areas and lines between adjacent stations were drawn on a map of the area by using Arc GIS 9.3 software with Arc tool box extension.

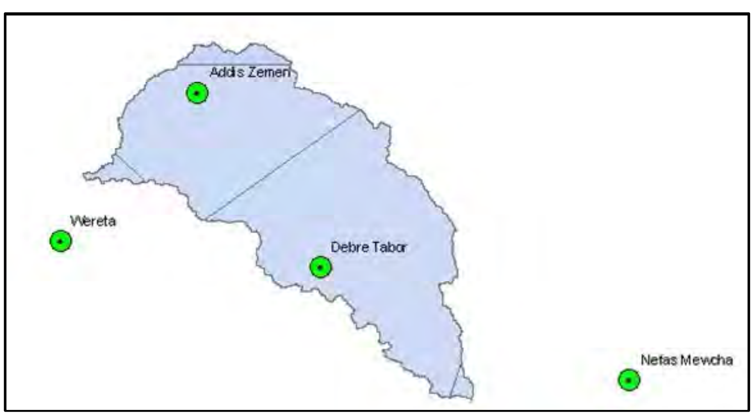

Figure 6: Thiessen polygon created from stations near Ribb

The perpendicular bisector of these lines forms a pattern of polygons with one station in each polygon. The area with which each station is taken represents the area of its polygon, and this area is used as a factor for weighting the station precipitation. The contribution of the rainfall from each gauging station is limited by its weighing factor.

According to Thiessen, the average rainfall, R_{areal} over the area can be computed from:

$$Rareal = \sum_{i=1}^{n} \frac{RiAi}{At}$$

Where, R_i is the rainfall at station i, A_i is the polygon area of station i, A_t is total catchment area, and n is the number of stations.

The area functions $A_{i/}A_t$ are known as the Thiessen coefficients and once they are determined for a given stable station network, the areal rainfall can be computed for the set of rainfall measurements.

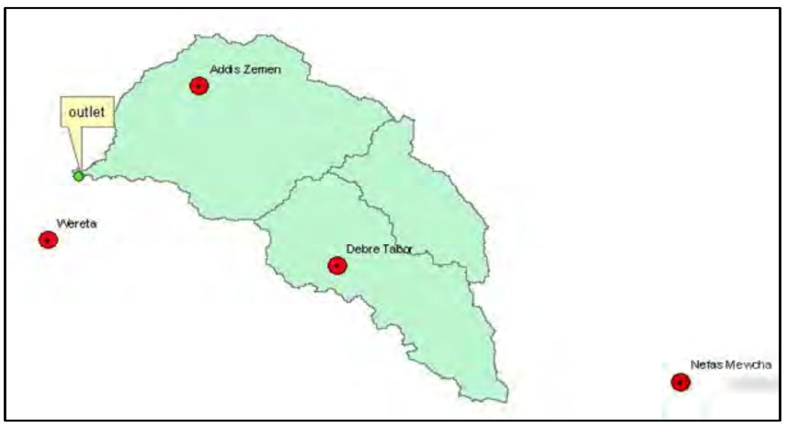

Figure 7: Rainfall stations and out let location

S.No.	Station Name	Period of records (years)	Elevation (m.a.s.l)	Latitude (Degree & Min.)	Longitude (Degree & Min.)	Mean Annual rainfall (mm)
1	Addis Zemen	21	1,850	$12^{0}12^{l}$	$37^{0}87^{l}$	851.5
2	Woreta	17	1,980	$11^{0}92^{l}$	$37^{0}68^{l}$	1035
3	Debretabor	27	2,690	$11^{0}88^{l}$	$38^{0}03^{l}$	1076
4	Nefas Mewucha	16	3,000	$11^{0}75^{l}$	$38^{0}45^{l}$	1210

Table 1: Station location and their respective length of records

gage name	Period of record	Catchment Area	Location		Mean Annual max Discharge
	Years	Km^2	Lat.	Long.	m^3/s
Ribb	1959-2006	1592	12.12	37.72	52

Table 2: Location of Ribb gauging station

3.5 Flow data

The daily discharge of the study area is collected from the Ministry of Water and Energy. Unlike the daily precipitation, the daily discharge has full data composition for the considered stations to represent the study area. The discharge gage is located near Addis Zemen where the downstream end is considered flood prone area.

3.6 Data filling and consistency

Missing flow data records for the sub basin is filled by developing correlation between the station with missing data and any of the adjacent stations with the same hydrological features and common data periods. Consistency and extension of flow data is analyzed by regression technique. The correlation equations used for Ribb gauging station in terms of Gumera gauging station, which shows good correlation is expressed below.

	GA	Gumera	Koga	Megech	Rib
GA	1	0.69	0.66	0.3	0.72
Gumera	0.69	1	0.59	0.33	0.74
Koga	0.66	0.59	1	0.25	0.64
Megech	0.3	0.33	0.25	1	0.34
Rib	0.72	**0.74**	0.64	0.34	1

Table 3: Correlation between Ribb and other nearby Rivers.

	Rib	Gumera
Rib	1	Y=0.3203X+2.1373
Gumera	2.3099X+3.7835	1

Table 4: Equation relating the Gumera flows with the Ribb River flow.

$$R = 0.32 * G + 2.1373$$

Where R= missed flow value at Ribb gage

G= flow value at Gumera gage

3.7 Hourly time series data availability and filling

The hourly precipitation processing doesn't follow the same procedure as the daily precipitation does. This may be because of various cases. The absence of sufficient hourly gauging stations (synoptic stations) in the area is the major problem. The presence of hourly precipitation data at Bahir Dar gaging station is not enough to execute the hydrologic model for the study.

An hourly discharge data is also another problem. Although daily missed flow can be filled out by regression equation relating the neighboring station to the gage in study, the hourly consideration doesn't hold true. For this research work the discharge data is developed from the rating curve. The rating curve developed as:

$$\mathbf{Q=a*(h'-h_o)^b}$$

Where **a** and **b** are constants, $\mathbf{h'}$= water surface level and $\mathbf{h_o}$=level of the ground at zero flow. Thus $\mathbf{h'-h_o}$= gage reading of depth of the water.

From the equation above,

$$Q=a*(h'-h_o)^b$$

$$\log(Q) = \log(a) + b*\log(h'-h_o)$$

Letting log (Q) =y and log $(h'-h_o)$ =x, and log (a) =c, a linear equation is developed with **b** slope of the linear graph, c intercept as;

$$y=c+bx$$

Relating the stage and discharge the following values was found (MoWE);

a=2.15092, b=2.786876, h_o=-3.609129

4. METHODOLOGY

4.1 Development of DTM

The key data element that GeoRAS uses to develop the input data is terrain data, commonly referred to as a Triangular Irregular Network (TIN). One source of data used to develop TIN is a Digital Elevation Model (DEM).

DEMs exist in grid (raster cell) format which can be displayed within ArcGIS, if the proper extensions are installed. The quality of this data is based on its resolution, or cell size.

The smaller the cell is, the greater the resolution and accuracy. However, the smaller the cell size, the greater the memory and computation requirements. The usefulness of DEMs for developing terrain models should be determined based on the cell size and the level of hydraulic analysis to be performed. The more approximate the analysis is to be, the greater the cell size that may be used. This can best be represented by TIN of the study area.

The TIN is generated from the spot heights acquired from different sources in ArcGIS which included:

1) GPS surveyed data collected along the two river banks, with good accuracy.

2) The spot heights of the flood plains taken from the surveyed data which extend approximately far from both the left and right bank stations and cover the floodplain if topography permits.

3) River bed cross section elevation data.

4.1.1. TIN of the study area

In one dimensional hydraulic modeling river and floodplain topography are represented as continuous surface. The representation of the river and floodplain is by the use of the TIN generated from the intersection of actual field data and the existing DEM of the study area. The TIN for this research is done with high precision due to the availability of the field surveys on the Ribb River channel which covers almost the entire reach.

The surveyed data contains information about the river layers (center line, right bank and left bank). The spot elevations are processed in ArcGIS to form shape files for the layers. When creating these shape files, there are meandering points which are lack of data for further processing. The points are then filled with successive interpolation and with additional field surveys.

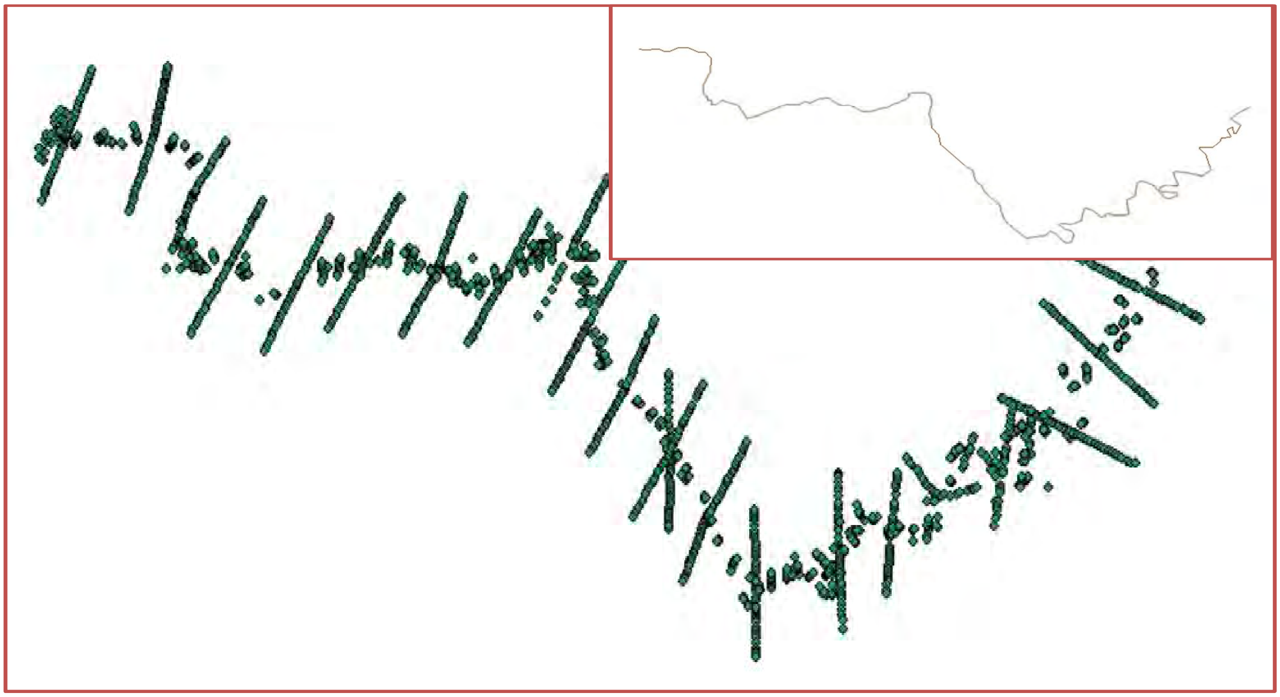

Figure 8 : Field survey points along the stream processed in ArcGIS

With the field survey processed in ArcGIS, shape file of the stream centerline and bank lines are created.

For high accuracy of stream and flood plain representation, a high resolution DEM is pre-requisite. Previous works on the area are carried out by using DEM 90. But this may not give appropriate result as required. In this paper DEM 30 is used to create TIN. The DEM is then intersected with field data to have greater accuracy for construction of river topography and other properties. The TIN is done with high precision due to availability of field data which covers most part of the stream and the flood plain stretch.

The TIN processed is assumed to represent the entire floodplain. From the approach the elevation values derived from the DEM is used to represent flood plain where as the values from actual field survey to river channel. This is because of the fact that there may be water flowing during the DEM processing.

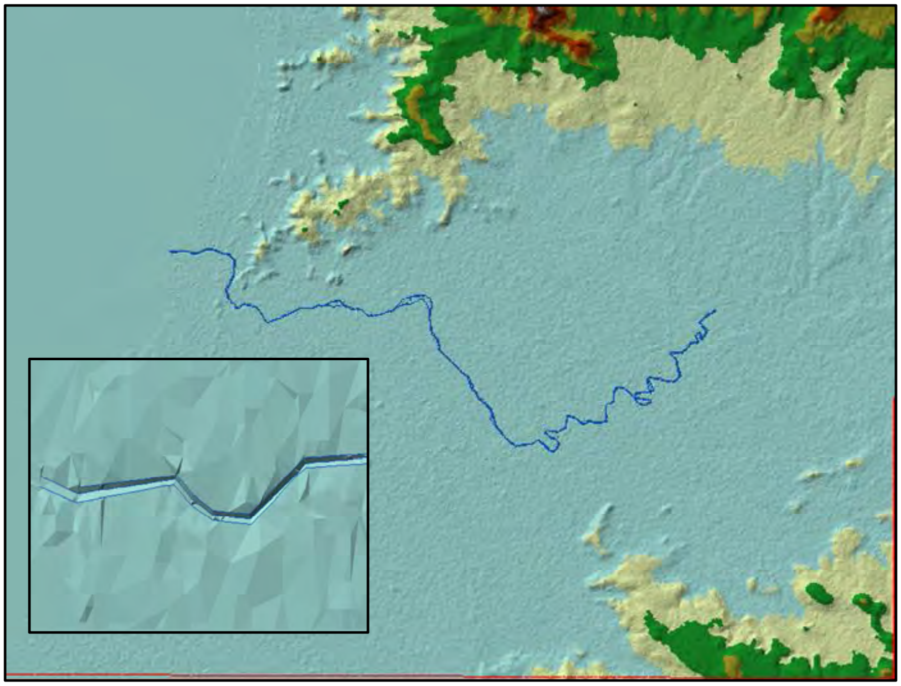

Figure 9: TIN of the study area and a close-up view of a portion of it.

4.2. Terrain Processing using Arc Hydro and HEC-GeoHMS

HEC-GeoHMS

HEC-GeoHMS is a set of ArcGIS tools specifically designed to process geospatial data and create input for the HEC-HMS. HEC-GeoHMS provides the connection for translating GIS spatial information in to model files for HEC-HMS. The GIS capability is for data formatting, processing and coordinate transformation. Currently, HEC-GeoHMS operates on DEM to derive sub-basin delineation and to prepare a number of hydrologic units. HEC-HMS supports these hydrologic inputs as starting point for hydrologic modeling. In this paper it is intended to derive parameters like: Curve Number, Basin Lag, and Time of concentration and Loss.

Terrain Processing Using Arc Hydro

The first step in doing any kind of hydrologic modeling involves delineating streams and watersheds, and getting some basic watershed properties such as area, slope, flow length, and stream network density. Traditionally this was (and still is!) done manually by using topographic/contour maps. With the availability of digital elevation models (DEM) and GIS tools, watershed properties can be extracted by using automated procedures. The processing of DEM to delineate watersheds is referred to as terrain pre-processing. There are several tools available online for terrain pre-processing.

In this study, we will use Arc Hydro (tools version that works with Arc-GIS 9.3) to process a DEM to delineate watershed, sub-watersheds, stream network and some other watershed characteristics that collectively describe the drainage patterns of a basin. The results from terrain processing can be used to create input files for many hydrologic models using HEC- Geo HMS.

All the steps in the Arc Hydro Terrain Pre-processing menu should be performed in sequential order, from top to bottom. The procedure followed for terrain processing using Arc Hydro is explained under using 30x30 DEM extracted for the respective sub basins and river feature class of the study area. For simplicity the main the main steps undertaken by arc hydro processing are; - DEM reconditioning, Fill sinks, Flow direction, Flow accumulation, Stream definition, Stream segmentation, Catchment grid delineation, Catchment polygon processing, Drainage line processing, Drainage point processing, longest flow path for the catchment and Slope determination. The terrain processing result for the sub basin is shown below in Figure.

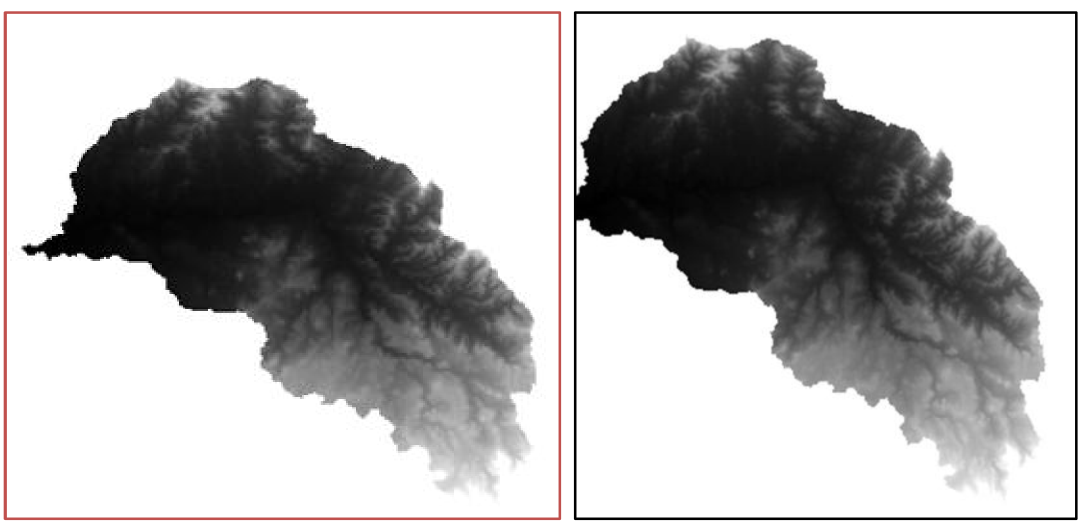

(a) (b)

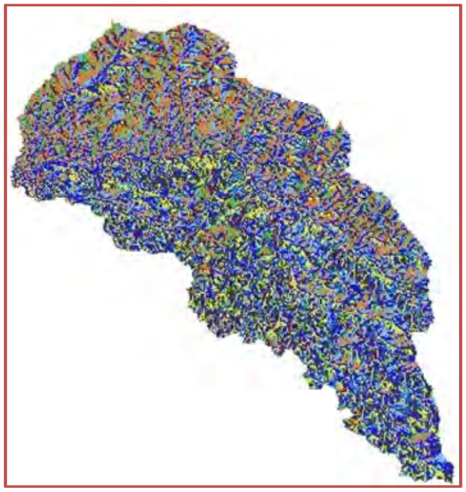

(c)

(d)

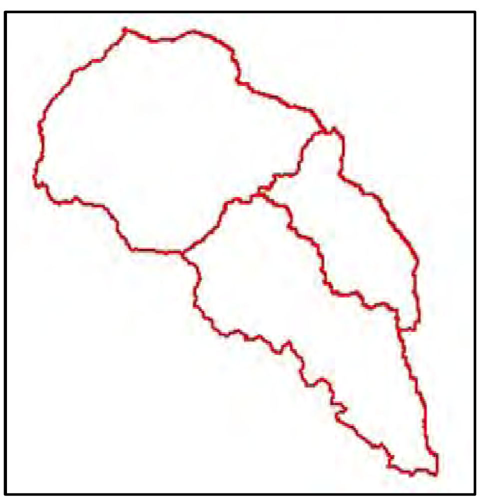

(e)

(f)

(g)

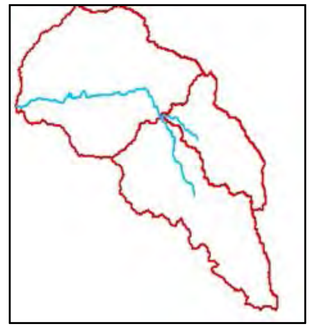

(g)

Figure 10**:** Terrain processing for Ribb sub basin using Arc hydro: a) Raw DEM b) Fill sink c) Flow direction d) Flow accumulation e) Catchment polygon processing f) polygon grid delineation g) longest flow path of catchment h) HMS Legend and Schematic.

The output from terrain processing in Arc Hydro is not only delineation and schematic for the catchment but also extraction of basin characteristics from physical properties of the catchment. Among the basin characteristics soil and land use are the major ones. According to the output of the model the following parameters are generated.

Component	Parameter	Unit	Value
Sub-basin 1	CN		73
	I_a	mm	17
	I_m	%	13
	A	Km^2	640.0
Sub-basin 2	CN		72
	I_a	mm	20
	I_m	%	14
	A	Km^2	218.5
Sub-basin 3	CN		73
	I_a	mm	22
	I_m	%	13
	A	Km^2	448.1
Reach 1	Lag	Min	210
Reach 2	Lag	Min	100
Reach 3	Lag	Min	390

Table 5: Catchment characteristic parameters extracted with Arc Hydro

5. MODELING

5.1. Overview of model simulation

Data models are central to the application of information technology because they are the means by which the real world is represented inside a computer.

The model starts with data processing and acquisition of the HEC-HMS. The data required for the model is derived from different hydrological components. This hydrologic representation imported into HEC-HMS is then combined with precipitation data and control specifications to create flow and time series data for use in a Hydrologic Data Model HEC-HMS. The flow and time series data from HEC-HMS is imported into the hydraulic model HEC-RAS along with its geometry data to develop water surface profiles. To close the loop, data is then once again used in ArcGIS with a Hec-GeoRAS extension from HEC-RAS to create a visual model used to delineate floodplain.

5.2. Hydrologic modeling with HEC-HMS

HEC-HMS modeling may be taken considering different time series values such as daily, hourly, annually and even in minute. Accuracy of the model output is high if it is in reverse order. Although most flood studies are undertaken considering hourly time steps, there are cases where daily data are taken. In this paper both daily data by gage weight method and frequency storm method are considered to compare the output result for each. The first portion covers modeling on daily basis.

The hourly data for the study area has only precipitation and flow value for one month. The rainfall has a full data for Bahir Dar station only thus making the result unreliable. Consequently, HEC-HMS outputs considering daily data using gage weight method and frequency storm method are used for further modeling approaches. Then the model output is compared with frequency analysis results which are selected by software called easy fit.

5.3. Modeling by daily data

5.2.1. Input data and model components

The main input data used for HEC-HMS are: areal precipitation, Evapo-transpiration (optional), observed flow, base flow and different watershed characteristics obtained from different sources.

An HEC-HMS simulation is defined by three components: the Basin Model, the Meteorological Model, and the Control Specifications. The Basin Model contains a schematic consisting of any combination of the seven objects (sub-basin, reach, junction, source, sink and reservoir).

The Basin Model stores information about the properties and connectivity of the objects in the schematic. In this research paper only the first three components are used.

The Meteorological Model contains time series information consisting of rainfall and evaporation data (optional). These data are associated with rain gages that the user defines in the Meteorological Model. The Control Specifications component defines simulation properties such as duration and time step.

The HEC-HMS model for the Ribb catchment is done considering and dividing the sub-basin in to three sub-catchments. The calibrated model is used for runoff generation for different frequency storms. In this research paper the gage weight method is selected. The weights are specified by using Theissen polygon created in ArcGIS9.3.

5.2.2. Modeling approach

5.2.2.1. Basin model

A general basin model consisting of sub-basin1, sub-basin2, and sub-basin3 is set up in HEC-HMS generated with ArcGIS for the study area. In addition to three sub-basins, an out let element is used in the basin model to relate the simulated flow to the historical observed total flow of the sub-basins. In this particular study for the respective sub basins, depending on the availability of time and data requirement , simulation is done with Deficit and constant loss method, Clark unit hydrograph and Monthly constant base flow condition.

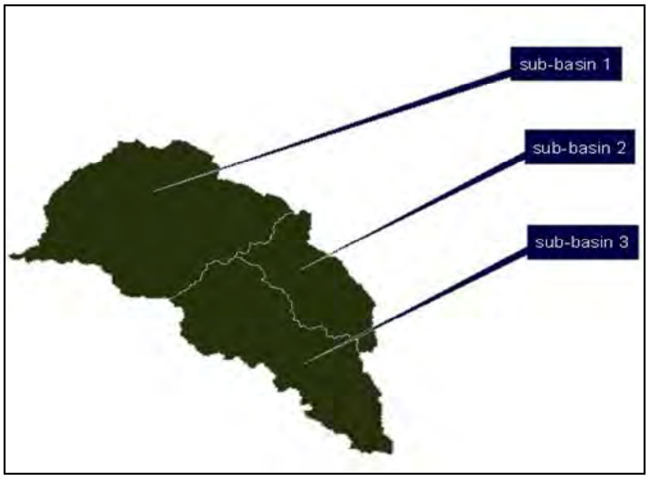

Figure 11 : Sub-basins of the Ribb catchment

Sub-basin	Area(km^2)	Contributing RF station
Sub-basin 1	640	-Woreta -Addis Zemen -Debretabor
Sub-basin 2	218.5	-Debretabor
Sub-basin 3	448.04	-Debretabor -Nefas Mewucha

Table 6: Ribb sub-basin area and contributing rainfall station

There are a total of four station used to represent the catchment. The stations are selected depending on their relative position to each sub-basin, data availability and the area they cover with respect to others.

Loss determination

The term loss refers to the amount of rainfall infiltrated into the soil. HEC-HMS supports the most common methods for calculating losses–such as initial/constant, SCS Curve No., gridded SCS Curve No., and the Green and Amps, and provides a moisture depletion option for simulations over extended periods of time.

In this paper for gage weight method the deficit and constant rate loss method is chosen because it has been used for long term simulations and also it is “mature” model that has been used successfully in many studies throughout the US (USACE, 2003), easy to set up and use, and not too much demanding in terms of data where much is missing in the study area.

Transform method

Runoff transformations convert excess precipitation on a sub-basin to direct runoff at the sub-basin outlet. Again, HEC-HMS allows runoff transformation determinations using lumped or linear distributed approaches.

Similarly, the Clark’s Unit Hydrograph model for direct runoff computation was chosen because of not only due to simplicity and minimum data requirements but also it gives a good performance than the other modules. In addition, it is suitable for conceptual models to transform rainfall to runoff process. The HEC-HMS is a conceptual model in which the process during simulation cannot be observed. It only gives the final output from the given input. The surface runoff calculations were performed using Clark Unit Hydrograph method which requires time of concentration to be computed for implementation.

A sub-basin element conceptually represents infiltration, surface runoff, and subsurface processes interacting together. The actual infiltration calculations are performed by a loss method contained within the sub-basin. All of the possible loss methods in HEC-HMS conserve mass. That is, the sum of infiltration and precipitation left on the surface will always be equal to total incoming precipitation. Thus effective rainfall is generated from the catchment loss and total rainfall on it.

Base flow

With regard to base flow, Constant monthly base flow method was used for its suitability to the study areas. The initial value before calibration was taken as the average of minimum flow.

Sub basin ↓	J	F	M	A	M	J	J	A	S	O	N	D
1	1.5	2.9	3.4	4.8	4.8	5.2	5.5	22	13.6	9.6	9.2	2.4
2	1.2	1.4	1.6	1.8	2.4	3.2	9.4	14	10.3	8.3	3.7	0.5
3	0.9	1.2	1.3	1.2	2.0	2.2	4.4	13	5.1	3.6	1.2	0.8

Table 7: base flow for the three sub-basins

Routing method

Muskingum routing is used to route the channel for continuous hydrological modeling. Automated calibration (optimization) was found to give optimum and reliable model parameters.

The objective function used for automated calibration (optimization) is the Peak-Weighted RMS Error. The HEC-HMS model has two optimization algorithms: Univariate gradient and Nealder and Mead search algorithm. Nealder and Mead search algorithm is used for this study. The optimization is made at the out let because the only observed flow is near the gage.

The parameters optimized is then used to represent the entire catchment and calibrated accordingly. This may be due to the smaller area of the Ribb catchment and the similarity in land use of the study area.

5.2.2.2Meteorological Model

Gage weight Method Inputs

The gage weight method is a meteorological method used in meteorologic model to produce a runoff from given timely precipitation data. The method requires the following inputs: sub-basin, gage precipitation and gage weights (temporal and spatial). Using the Thiessen polygon, the stations used to represent each sub-basin are tabulated here under.

Sub-basin/station		Spatial/depth weight	Time/seasonal weight
1	Woreta	0.05	0.05
	Addis Zemen	0.8	0.9
	Debretabor	0.15	0.05
2	Debretabor	1.0	1.0
3	Nefas Mewucha	0.85	0.95
	Debretabor	0.15	0.05

Table 8: Rainfall stations near Ribb

5.2.2. Model calibration

According to the Canadian Foundation for Climatic and Atmospheric sciences (CFCA), a single event hydrologic modeling should be used for simulating storm and frontal rainfall induced floods. Continuous modeling approach should be then employed for snow melt and mixed rainfall snowmelt flooding, as well as for simulating the prolonged periods of summers of low flows.

The value of each parameter found in HEC-HMS must be specified to use the model for estimating runoff volume and routing hydrographs. Some of the model parameters can't be estimated by observation or measurement of the watershed characteristics. For example the parameter '**x**' and '**k**' in the Muskingum routing model can't be measured but can be estimated approximately for limited cases.

How then can the appropriate values for the parameters be selected? If rainfall and stream flow observations are available, calibration is the answer. Calibration uses observed hydro meteorological data in a systematic search for parameters that yield the best fit of the computed results to the observed runoff.

This search is often referred to as optimization. Optimization begins from initial parameter estimates and adjusts them so that the simulated results match the observed stream flow as closely as possible.

To compare a computed hydrograph to an observed hydrograph, the program computes an index of the goodness-of-fit.

Algorithm included in the program search for the model parameters that yield the best value of an index, also known as objective function. Out of four objective functions in HMS, Peak-weighted root mean square error is selected for this study.

This function is an implicit measure of comparison of the magnitudes of the peaks, volumes, and times of peak of the two hydrographs. Nelder and Mead Algorithm method of search parameter that minimizes the value of the objective function is used for this study. This algorithm relies on a simple direct search.

A total of 15 years historical data from 1992 to 2006 is used, calibration (1992- 2001) and validation (2002-2006) for the selected watersheds of the sub basins. Manual and automatic calibration was used for optimization of observed and simulated flow data using initial parameter from watershed characteristics. Calibration was done by taking initial parameters generated from HEC-GeoHMS and ArcHydro for the catchment. With the initial parameters, the calibration was then processed until the simulated value resembles the observed data.

5.2.3. Model efficiency/performance

The performance of a model must be evaluated on the extent of its accuracy, consistency and adaptability (Goswami, 2005). A forecast efficiency criterion is therefore necessary to judge the performance of the model.

Assessing performance of a hydrologic model (Base, 2005) requires subjective and/or objective estimates of the closeness of the simulated behavior of the model to observations.

For the Ribb catchment study, model simulation has been evaluated using efficiency criteria such as coefficient of determination (R^2) and [Nash and Sutcliff (E_{NS}), 1970].

The R^2 coefficient and E_{NS} simulation efficiency measure how well trends in the measured data are reproduced by the simulated results over a specified time period and for a specified time step. The range of values for R^2 is 1.0 (best) to 0.0. The statistical index of modeling efficiency (E_{NS}) values range from 1.0 (best) to negative infinity.

The Nash and Sutcliff (E_{NS}) efficiency equation is given by

$$E_{NS} = 1 - \frac{\sum_{i=1}^{n}(q_{oi} - q_{si})^2}{\sum_{i=1}^{n}(q_{oi} - \overline{q}_o)^2}$$

And the standard R^2 is given by

$$r^2 = \frac{\left[\sum_{i=1}^{n}(q_{si} - \overline{q}_s)(q_{oi} - \overline{q}_o)\right]^2}{\sum_{i=1}^{n}(q_{si} - \overline{q}_s)^2 \sum_{i=1}^{n}(q_{oi} - \overline{q}_o)^2}$$

Both efficiency evaluation criteria parameters must resemble each other. For the Ribb case the **E_{NS}** has a value of 0.719 and **R^2**=0.72.

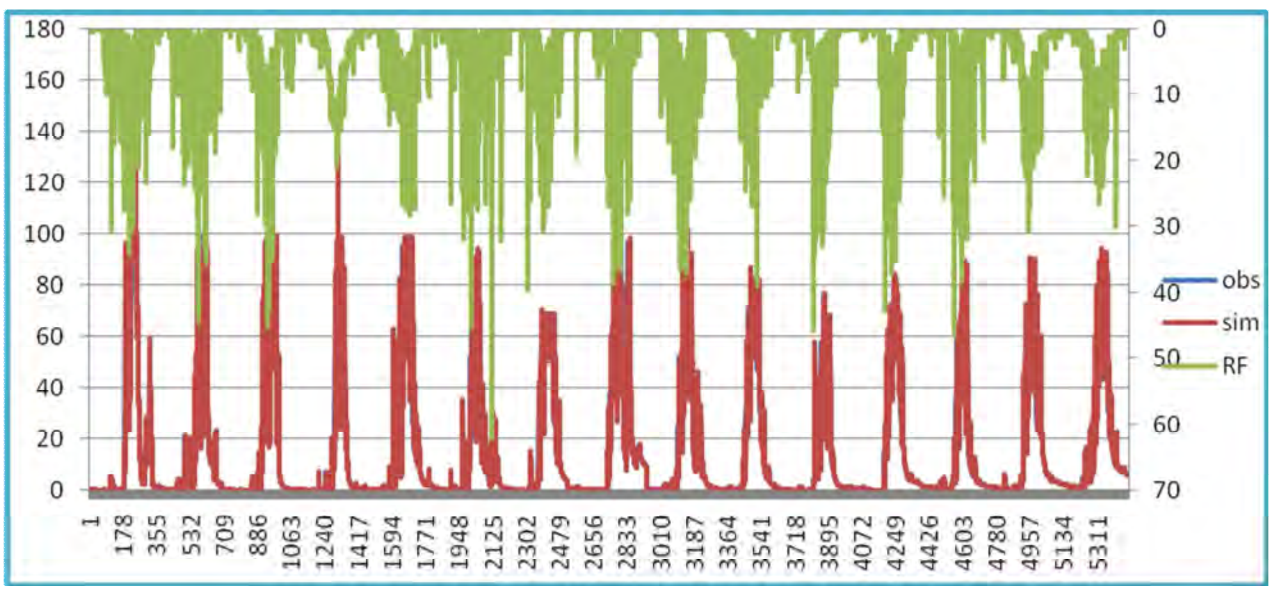

Figure 12: Calibrated model output (daily time series)

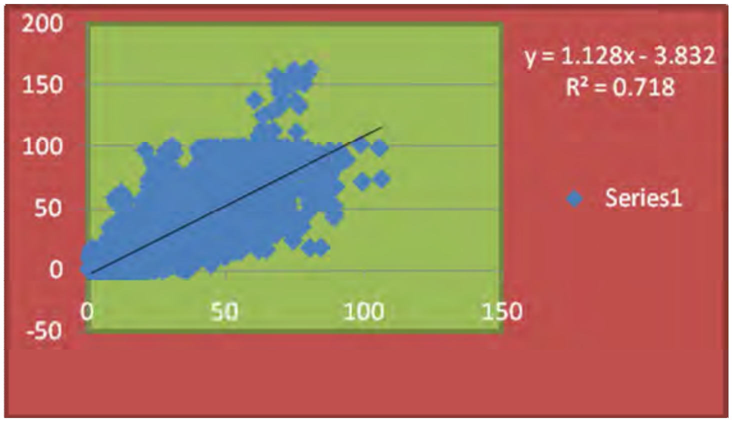

Figure 13: Correlation between observed vs. simulated flow

The model performance is validated accordingly. For the HEC-HMS model there are a total of 15 years taken for both calibration and validation. The validation time was selected as the last five years of the total years.

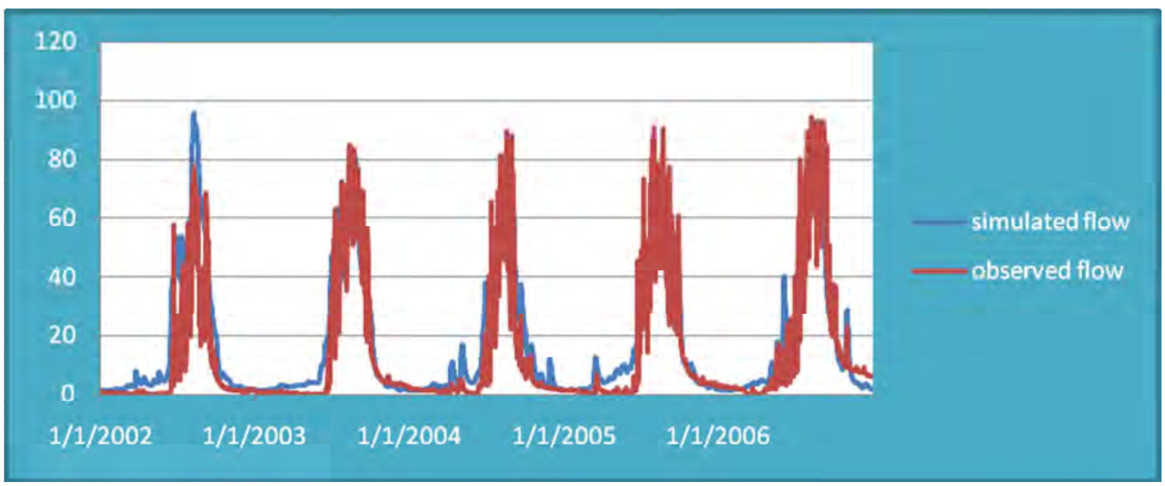

Figure 14: Simulated vs. observed (daily)

The following table shows final output of HEC-HMS using daily time series data.

Yr	92	93	94	95	96	97	98	99	2000	2001
Q	163.2	99.93	99.5	137.7	98.6	94.5	70.2	99	101.8	86.9

Table 9: HEC-HMS output of daily time series

The above peak values obtained from HEC-HMS are the results of the following optimized parameter:

Component	Parameter	Unit	Initial	Optimized
Subbasin-1	Clark Storage Coefficient	HR	120	120.84
Subbasin-1	Clark Time of Concentration	HR	32	32.609
Subbasin-1	Constant Rate	MM/HR	4.5	4.5
Subbasin-1	Initial Deficit	MM	0.5	0.5
Subbasin-1	Maximum Deficit	MM	45	45
Subbasin-2	Clark Storage Coefficient	HR	34.148	10.118
Subbasin-2	Clark Time of Concentration	HR	28	25.826
Subbasin-2	Constant Rate	MM/HR	4.5	4.5
Subbasin-2	Initial Deficit	MM	0.5	0.5
Subbasin-2	Maximum Deficit	MM	45	45
Subbasin-3	Clark Storage Coefficient	HR	120	75.295
Subbasin-3	Clark Time of Concentration	HR	30	27.671
Subbasin-3	Constant Rate	MM/HR	4.5	4.5
Subbasin-3	Initial Deficit	MM	0.5	0.5
Subbasin-3	Maximum Deficit	MM	45	45
Reach-1	Muskingum K	HR	34	14.513
Reach-1	Muskingum X		0.13	0.11991
Reach-2	Muskingum K	HR	39	4.8338
Reach-2	Muskingum X		0.15	0.0435556
Reach-3	Muskingum K	HR	32	48.683
Reach-3	Muskingum X		0.15	0.13836

Table 10: Optimized parameters of HEC-HMS for Ribb catchment

5.4. Modeling by frequency storm method

With the input from HEC-GeoHMS and some edition from the main HEC-HMS, the model is simulated for rainfall intensity of 2, 10, 50, and 100 year return periods. The frequency intensity values are found from the Ethiopian Roads Authority drainage manual (ERA, 2002).

D(hr)	RF depth with return period			
	2	**10**	**50**	**100**
1	27	41.5	55.7	62.5
2	32	49.8	66.7	74.2
3	37	57.1	72.1	81
6	45	66.1	78	90
12	50.2	72	84	93
24	52	74	88	94

Table 11: IDF table for the study area (ERA Drainage Design Manual, 2002)

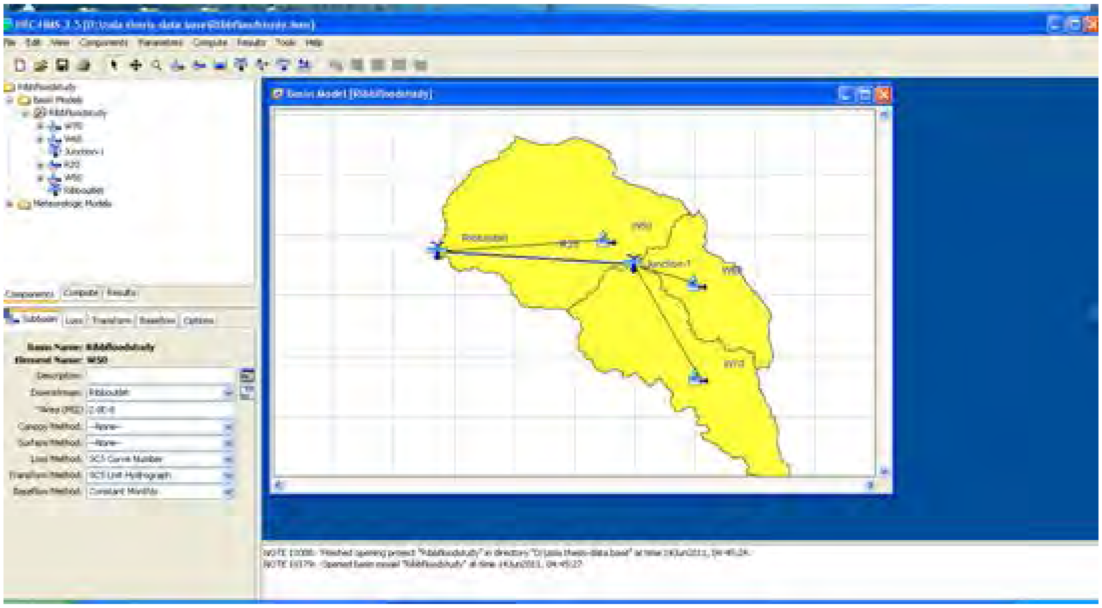

Figure 15: HEC-HMS schematic imported from HEC-GeoHMS

5.5. Output of HEC-HMS by frequency storm

The model has a capability to produce and generate values for different flow conditions (return periods). Given the above input parameters, the flow values are found accordingly. From the result table minimum peak flow for the Ribb River is occurred for 2 year return period for 24 hour storm duration and the maximum obtained with 100 year frequency storm for the same duration. The value being 91.8m^3/s and 308.4m^3/s for 2 year and 100 year frequency respectively.

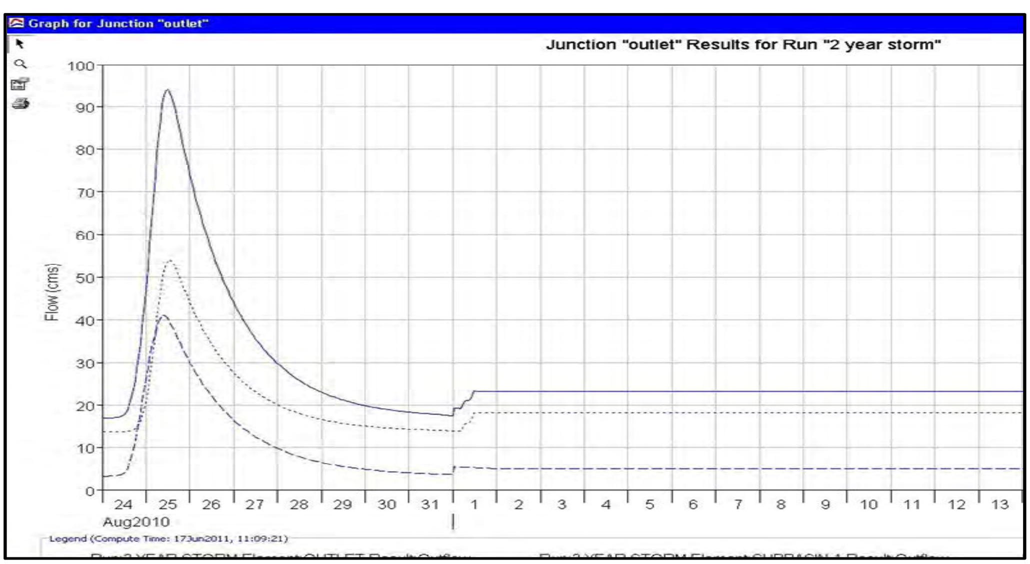

Figure 16 : 2 year flow hydrograph of Ribb River

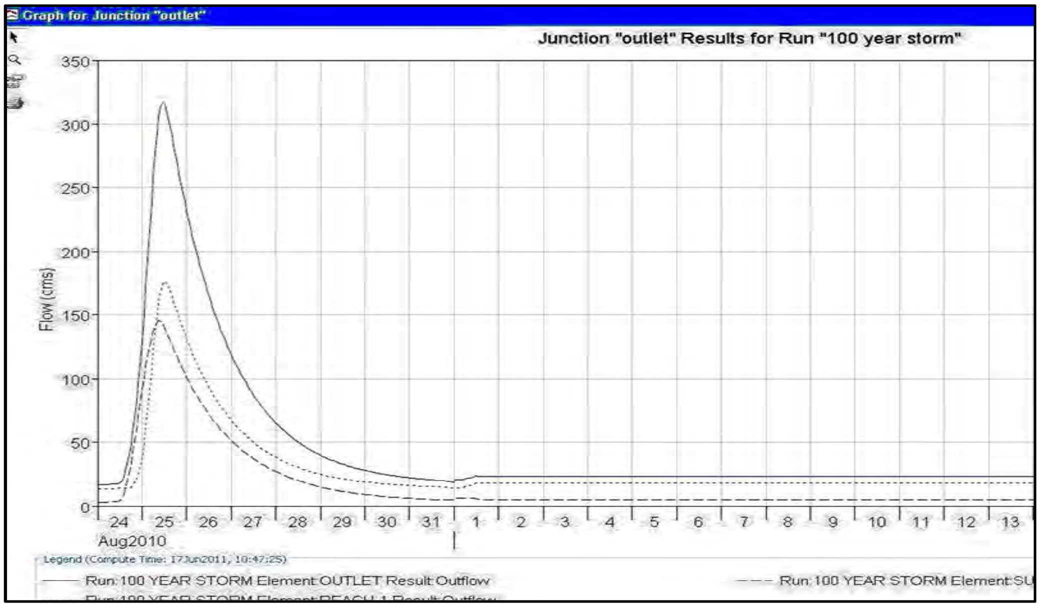

Figure 17: 100 year frequency stream flow hydrograph of Ribb River

And the overall frequency storm flow hydrograph is used to observe and compare each flow values.

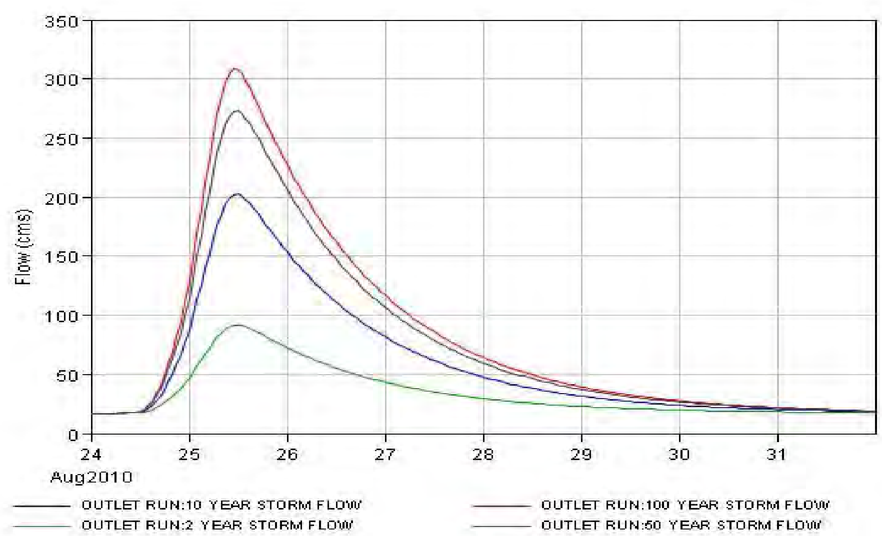

Figure 18: Frequency flow values of the Ribb River for 2, 10, 50 and 100 year storms.

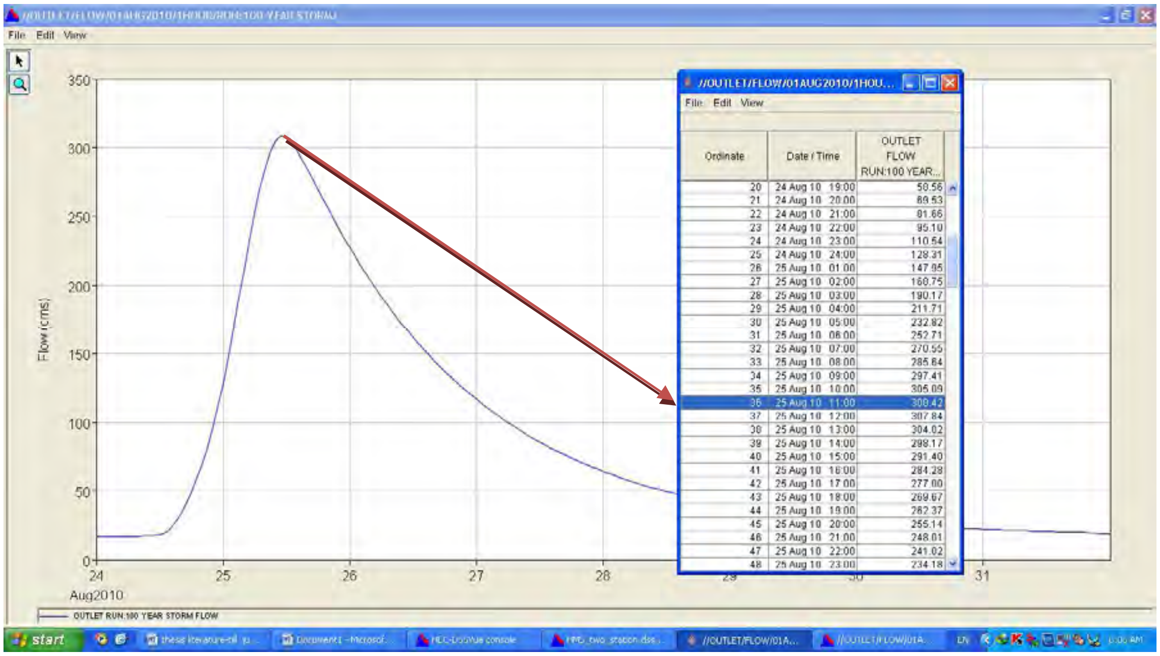

Figure 19 Time series output value for the respective hydrograph (HEC-DSS)

Finally the HEC-HMS model result is compared with the frequency analysis results considering different techniques. The methods applied in this paper are selected based on their efficiency and simplicity. But the primary criterion is their correlation with the simulated flow data of the Ribb River. They are selected using software called best fit for selection of methods. According to the output the following four popular methods are selected.

Method		Q_t (m^3/s)			
		2	10	50	100
FA	Gumbel	94.4	179.6	256	288.313
	Normal	99.706	129.5	147.45	153.821
	EVI	95.89	130.1	159.99	172.655
	LP3	91.33	127.25	176.12	201.613
HEC-HMS		91.8	202.4	273.1	308.414

Table 12: Comparison of flow values (frequency analysis and the HEC-HMS)

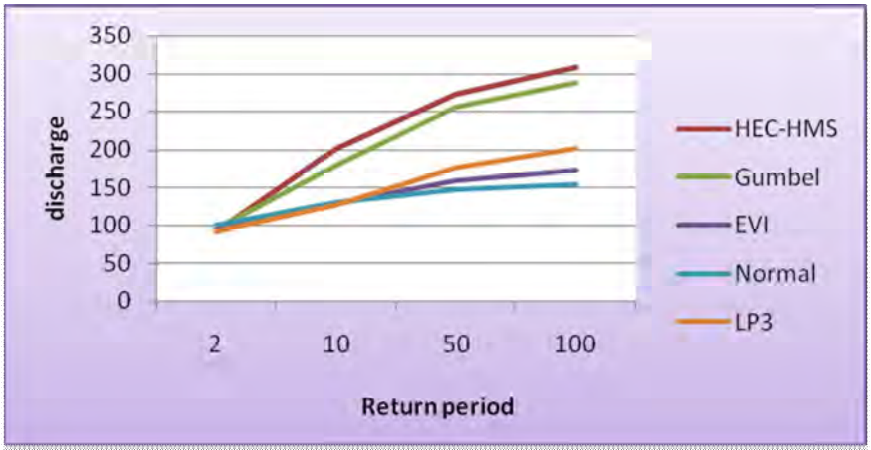

Figure 20: Comparison of the flow values of the Ribb River

In the above figure the frequency discharge value derived using Gumbel's method show high similarity to the HEC-HMS. The other three are much lower than the result of the HEC-HMS. In most flood study, either the model result or that found by the frequency analysis may be taken based on different considerations.

Previous studies and observations on the Ribb River shows there is high transportation, accumulation and concentration of sediment. This may be due to the nature of soil near the River which is very loose.

Frequent washing and sedimentation of the channel has the effect on the gage recoding of the river. The deviation on the gage reading due to this sedimentation and manual error results in less reliability of the historical data of the river.

For the above mentioned and other minor cases, the HEC-HMS result is taken as a good representation of discharge scenarios for studies on and around the area.

5.6. Hydraulic modeling with HEC-RAS

5.6.1 Input data and model components

One of the functions of the HEC-RAS program is to determine surface elevations at any point of interest. The data needed to perform these computations are separated into geometric data and steady flow data (boundary conditions). The input data for HEC-RAS is imported from ArcGIS which is discussed below.

Pre RAS processing using Hec-GeoRAS

The goal of this part was to develop the basic spatial data required to generate the HEC-RAS Geometry Import File. The process required is the Generation of a digital terrain model (in this paper TIN is generated from field data and the DEM of the study area), Definition of base 2D spatial features and Generation of 3D spatial data and HEC-RAS Geometry Import File. With the DTM/TIN generated earlier, the next step is 2D spatial feature definition.

2D Spatial Features Definition

With the digital terrain representation (TIN) created, the next step is to extract the geometric information required by HEC-RAS. This step started with the delineation of a series of 2D spatial features corresponding to the stream centerlines, the left and right bank lines, the flow paths, and the cross sections along the streams. The contour lines may be helpful in this regard if the resolution of the TIN is poor.

In general, the delineation of cross sections located close to river junctions was not easy: each cross-section had to cross the stream centerline exactly once, the bank lines exactly twice (left and right), and the flow paths exactly three times (left, right and centerline) and they should not intersect each other.

Cross section geometry

Boundary geometry for the analysis of flow in natural streams is specified in terms of ground surface profiles (cross sections) and the measured distances between them.

Cross sections should be perpendicular to the anticipated flow lines and extend across the entire flood plain (these cross sections may be curved or bent). For this research paper it is made to extend to about a total of 8km with 4km at each stretch of the floodplain.

Cross sections are required at locations where changes occur in discharge, slope, shape or roughness; at locations where levees begin or end and at bridges or control structures such as weirs.

Each cross section is identified by a Reach and River Station label. The cross section is described by entering the station and elevations (x-y data) from left to right, with respect to looking in the downstream direction.

The cross section for this research work is extracted both from field data and its counterpart digitized DEM/TIN. The study area TIN is made from the field survey data and the DEM of the area. During the extraction, the field data is assumed to represent the channel geometry than the DEM.

This is because of the fact that there may be water flowing during the processing of the DEM. On the other hand the resolution of the current DEM is less accurate for the river channel.

Although the DEM resolution is low for the channel, it is best representation for the flood plain. Integrating both data sources therefore has a greater accuracy than individual source.

Before digitizing the cross section the stream layers must be made available. The layers are; stream center line, flow path center line, flow path lines (left and right) and bank lines.

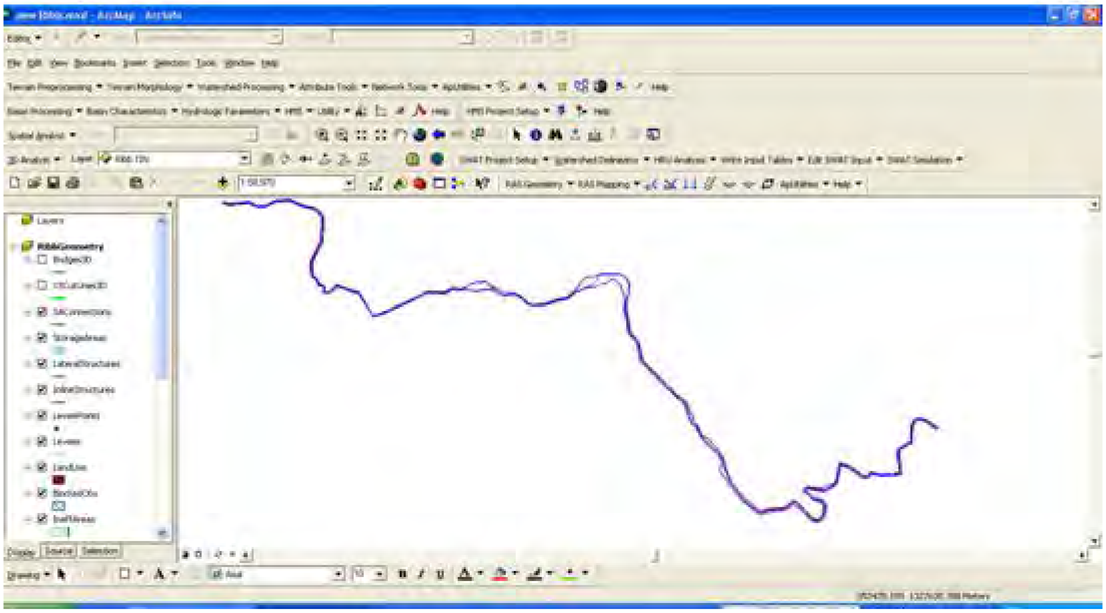

Figure 21: A digitized Ribb River with RAS layers

The above five features are extracted from prepared TIN of the study area. The TIN was generated from field survey of the area and DEM.

Accordingly actual field data are made to represent channel cross section where as the DEM to the flood plain. During digitizing shape files of the river or contour can be used to follow.

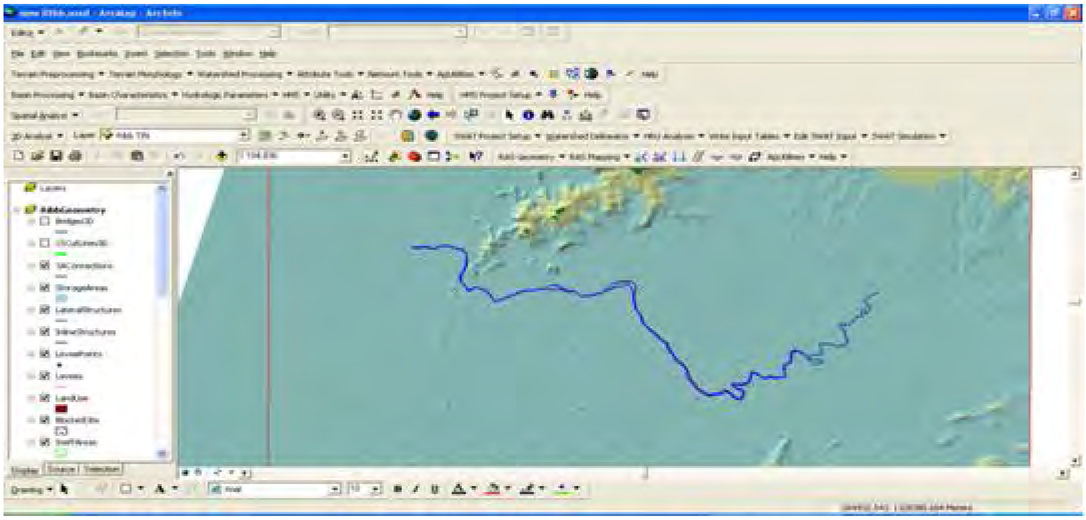

Figure 22: An underlying TIN and associated Ribb River

Preprocessing by Hec-GeoRAS in ArcGIS is the first step in the extraction processes. The step is used in geo-referencing and digitizing the stream layers for further use in HEC-RAS.

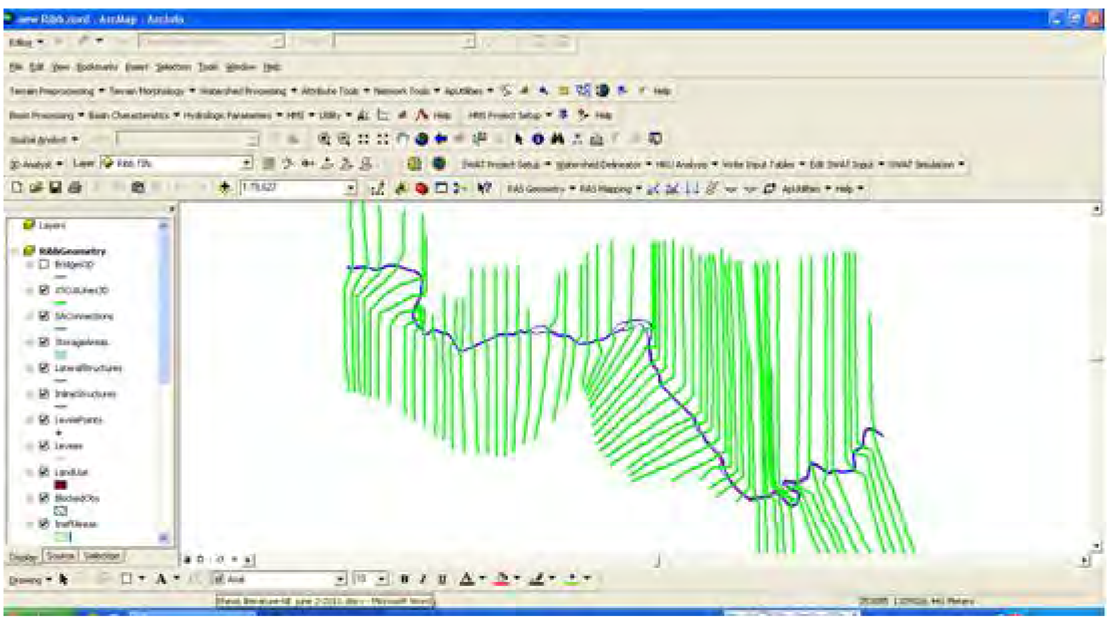

Figure 23: Cross section of the Ribb River digitized in GIS9.3

3D Spatial Features and HEC-RAS Geometry Import File Generation

The 3D spatial data generation involved creation of 3D stream centerlines and 3D cross-sections, with *Z* values to define elevations. The *Z* values were extracted from the TIN.

Once generated, the 3D features identified the stream network and the HEC-RAS model layout. The generated cross section is then changed to polyline *Z*. The 2D point data is changed to the 3D polyline due to the extraction of elevation from the DTM/TIN.

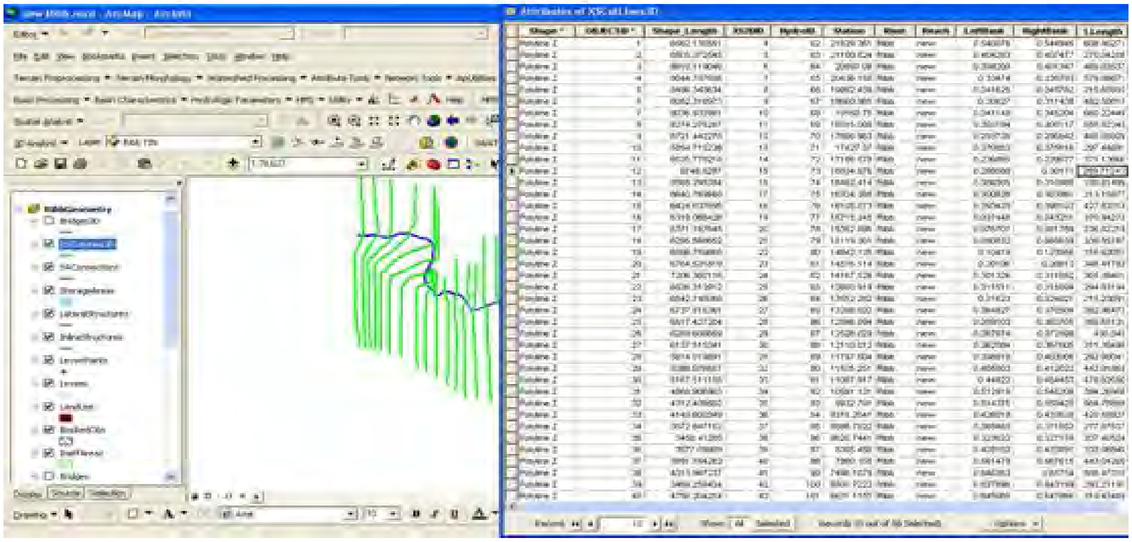

Figure 24: 3D spatial feature generated after extraction of elevation from TIN

5.6.2. Exporting to HEC-RAS

It is very important to edit and geo-reference all necessary layers in GIS. Although the HEC-RAS has an editing interface for the exported value, the GIS is a better way to reduce the error during post-RAS process (flood mapping and delineation). There are different options to leave or export RAS layers depending on their use and necessity. There may be errors during pre-RAS processes.

The bank stations which are made fit with the cross section points in GIS may not match when exported to HEC-RAS. In this case manual edition should be applied.

The exported cross section may not also be readable by the HEC-RAS. The problem may emerge from the unit system between the HEC-RAS and that used in GIS. The GIS unit system must be re-projected according to the RAS unit.

Since most GIS inputs such as DEM, TIN and field cross sections are in metric unit it must be projected to the same unit. In the figure below the last two cross sections bank points are away from the channel bank lines, so that they require manual edition.

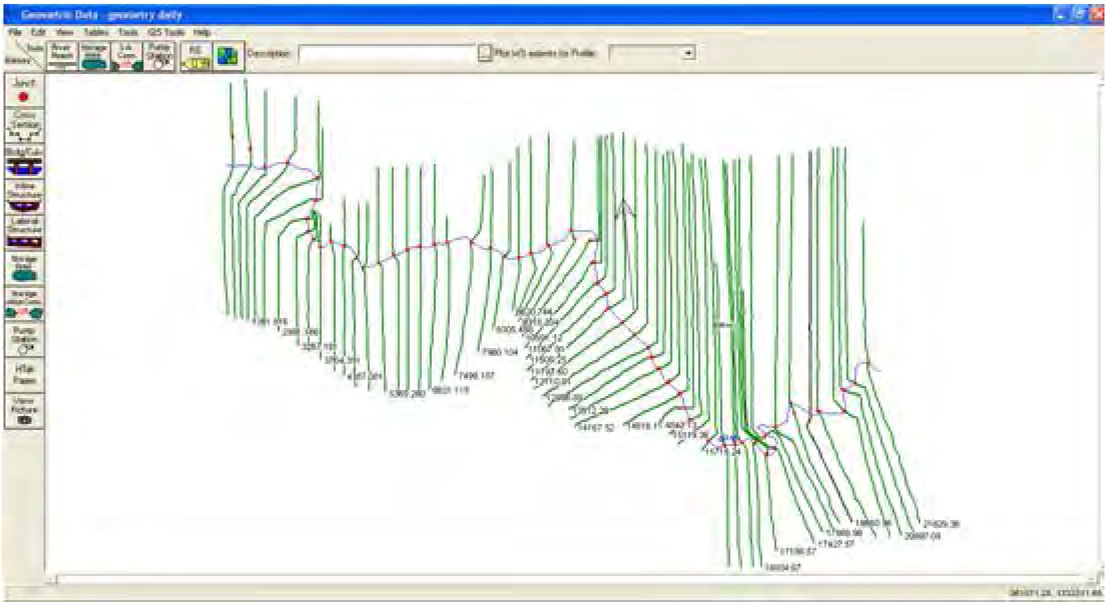

Figure 25**:** A cross section views in HEC-RAS geometric window imported from GIS.

The geometric data window edits not only the river sections but also structures associated with the river system. This structures may be; bridges/culverts, deck/roadway, weir structures, levees, dykes etc. These structures are also digitized and geo-referenced in GIS and exported to HEC-RAS for further editing.

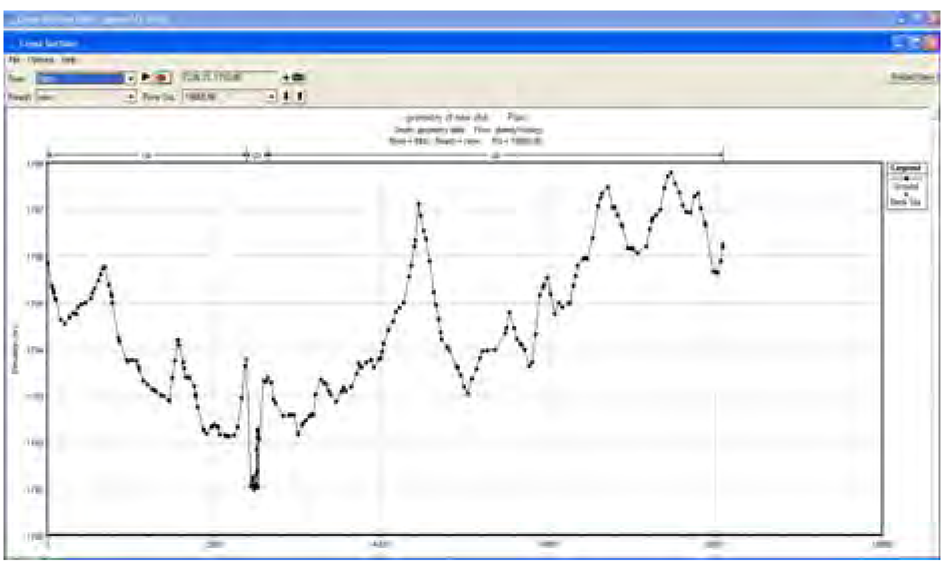

Figure 26**:** Cross section view at river station 14842.13 of the Ribb River channel

The structures such as bridges and culverts could not be extracted from the TIN. These structures were manually added to the model through the HEC-RAS interface. The available field information did not include every bridge or culvert along the stream network.

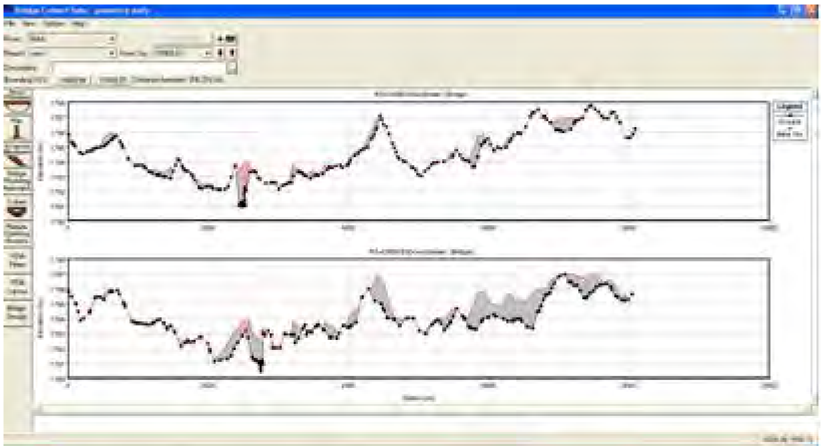

Figure 27: Bridge location at station 19500.63

5.6.3. Entering Flow data and boundary condition

The discharge values for different return periods can be entered either manually or connecting to the desired location (for the Ribb case out let near Addis Zemen) on HEC-HMS by exporting to HEC-RAS using HEC-DSS.

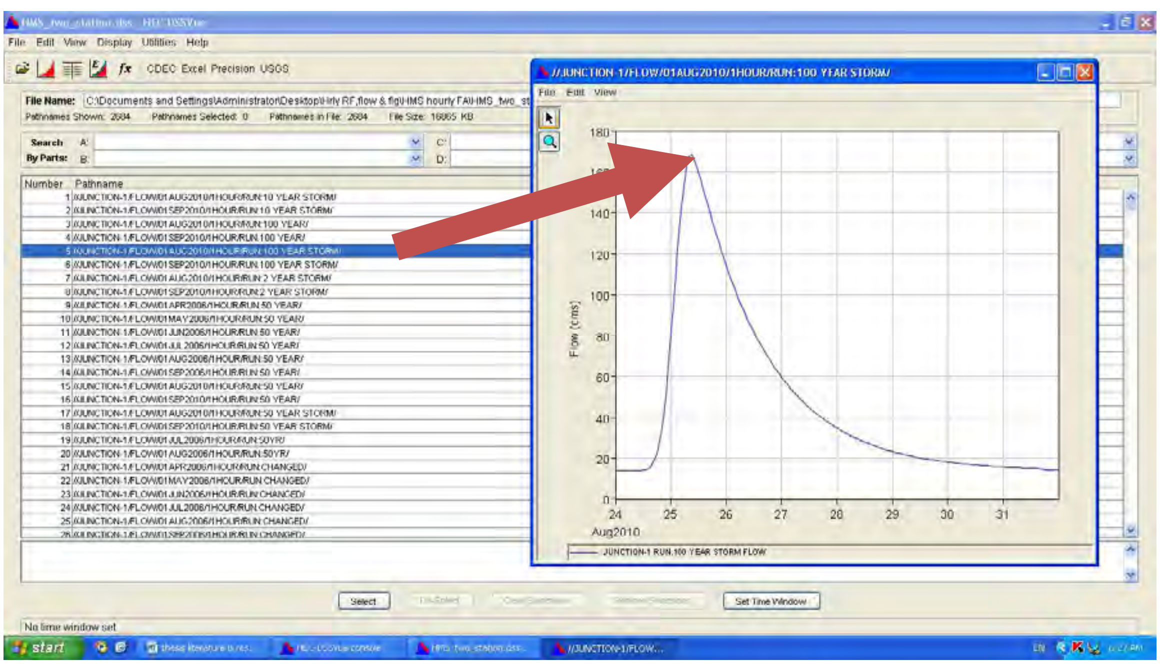

Figure 28: HEC-DSS view for exporting to HEC-RAS showing peak flow hydrograph

The roughness coefficients (Manning's coefficient) and boundary conditions were added to the model manually. The values selected were 0.035 and 0.041, for the stream channel and overflow banks, respectively.

The model was run for subcritical flow regime conditions and steady flow water surface profile computations. The iterative solution of the energy equation, using the standard step method, solved the steady flow, while Manning's equation and contraction/expansion coefficients determined head losses. The effect of the bridges and culverts was also determined by solving the energy equation. The calibration of the HEC-RAS was done by varying the cross section even though it is a complicated and time consuming process.

Before applying the computation process the model must be set up for boundary condition. There are various methods of boundary condition used. The method used in this paper is the critical depth at the downstream end of the reach. The model calculates the depth from the given elevation data and discharge. The water surface can also be used if the accurate and up-to-date value is available.

Finally the plan must be established for each model simulation. The plan has a user specified description and application.

5.7. HEC-RAS output

HEC-RAS requires flow and topographic data as channel and flood plain cross section. Given this two sets of data in appropriate form the resulting model efficiency is high. The model gives the food plain water surface profile in 2D view.

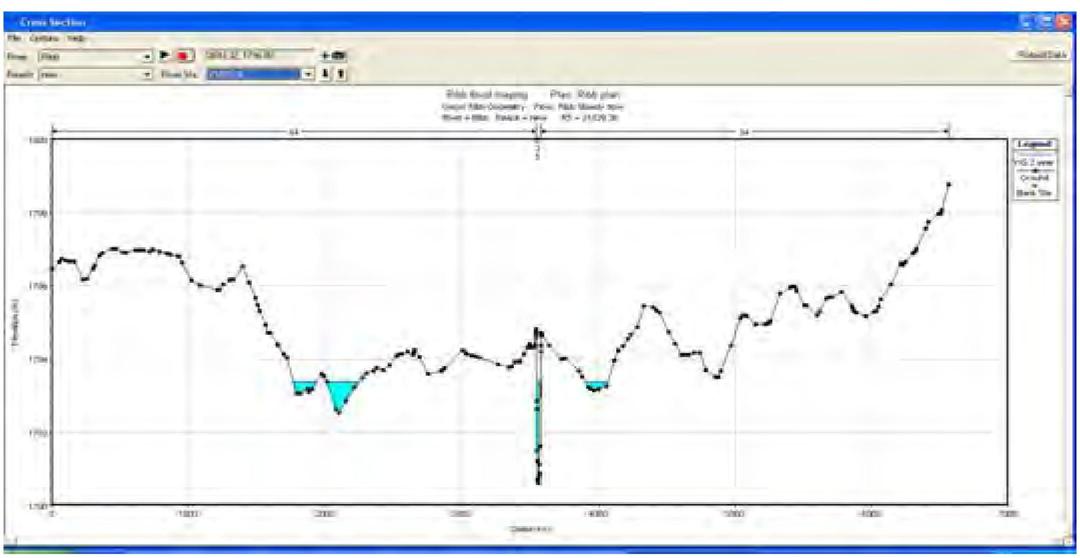

Figure 29: Cross section view at River station 21829.36 for profile #1(2 year return period)

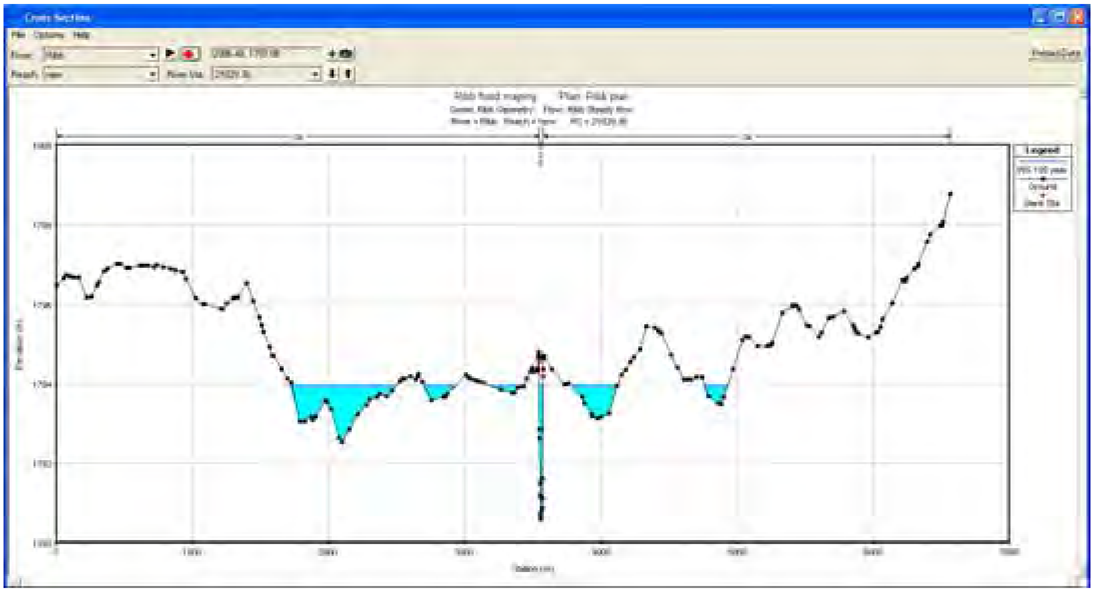

Figure 30: Cross section view at river station 21829.36 for profile #4(100 year storm)

In the output cross section view, the river channel is seen as v-shaped. In real case it shouldn’t be like that. This is because of the high stretch of the flood plain with respect to the channel width. One can simply observe the fact.

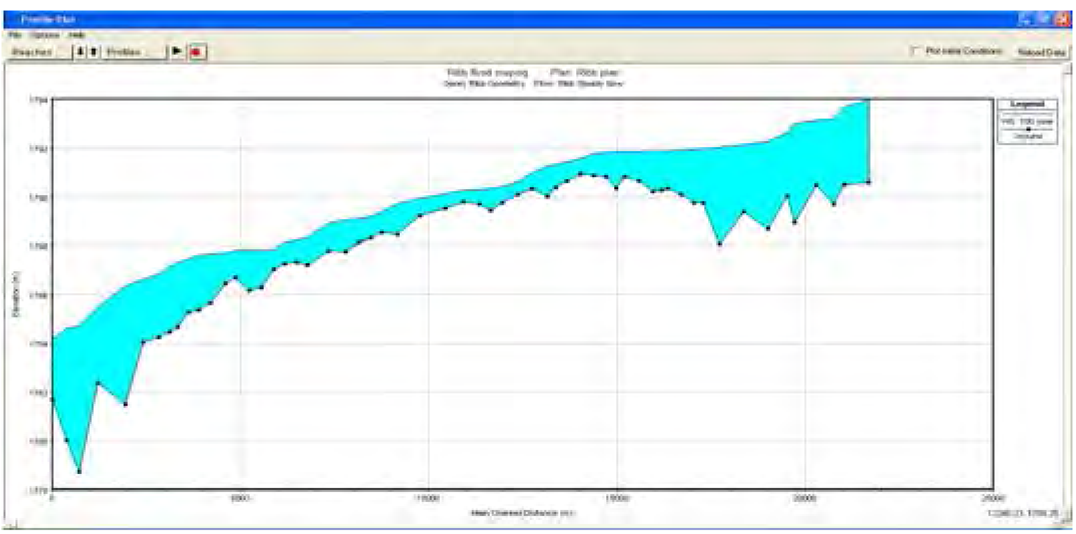

Figure 31: General profile plot of the reach for 100 year storm

Other application of HEC-RAS is providing the 2D river water profile to ArcGIS to display the flood plain in 3D. The flood plain mapping and finally delineated output is the one which uses the RAS output in the form of the river profile.

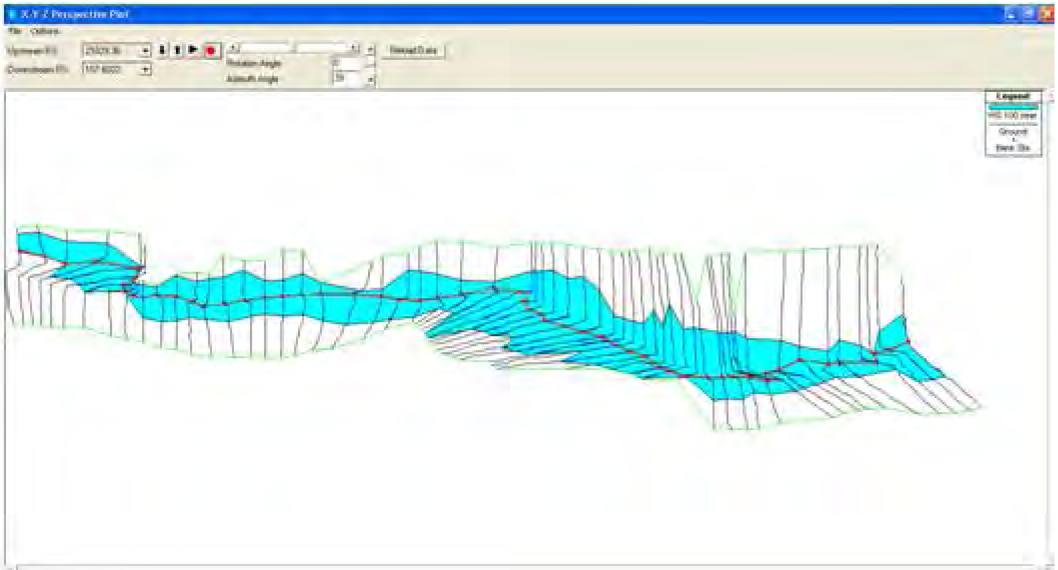

Figure 32: 3D perspective view of the flood plain and the channel in HEC-RAS (100 year storm)

Finally the output table for the model is given for each station consisting of different parameters. The parameters can be changed during calibration.

The HEC-RAS is calibrated for the cross section parameters only. This is because the flow data has already passed calibration and validation processes.

One of the difficult part or short coming of this model is its complexity during calibration. The availability and accuracy of cross section data may reduce the burden.

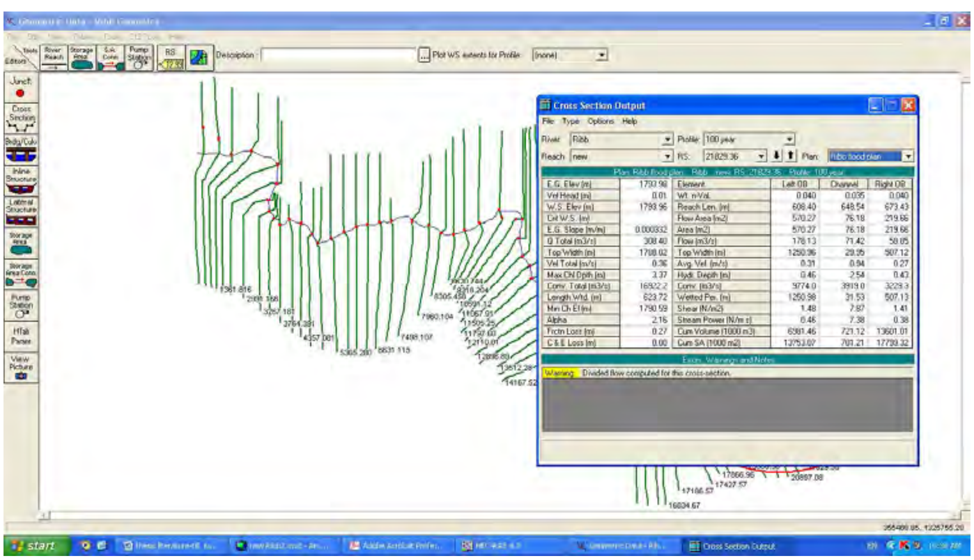

Figure 33: RAS output table at station 24120.95

5.8. Exporting HEC-RAS results and post-RAS processing

Once HEC-RAS computed values are completed with no errors, the next step is exporting the output to ArcGIS for post-RAS processing. Post-RAS processing is the one which uses HEC-RAS output for floodplain inundation mapping and delineation.

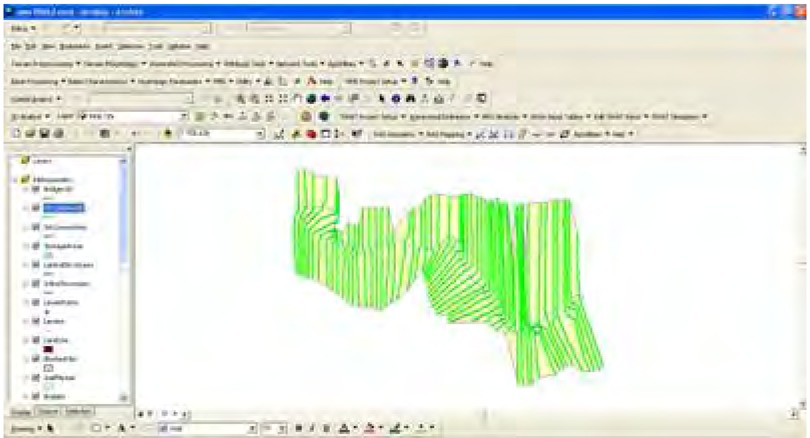

Figure 34: Bounding polygon for the water surface TIN generation

5.9. Flood plain delineation

Areas inundated by flooding occur wherever the elevation of the floodwater exceeds that of the land. To delineate these areas, we will create surface models of the floodwater and land surface, and then compare the elevations. Let's start with the floodwater model. HEC-RAS represents the floodplain as a computed water surface elevation at each cross-section.

During the data import step, these elevations were brought into ArcGIS, along with the distance from the stream centerline to the left and right floodplain boundaries. Hence, two things are known about the floodplain at each cross-section: water surface elevation and width on each side of the centerline.

5.10. Flood map

With the bounding polygon created (figure above), water surface TIN is created from the given profiles and underlying DTM/TIN. The water surface TIN consequently gives rise to flood plain delineation.

With the bounding polygon created (figure above), water surface TIN is created from the given profiles and underlying DTM/TIN. The water surface TIN consequently gives rise to flood plain delineation.

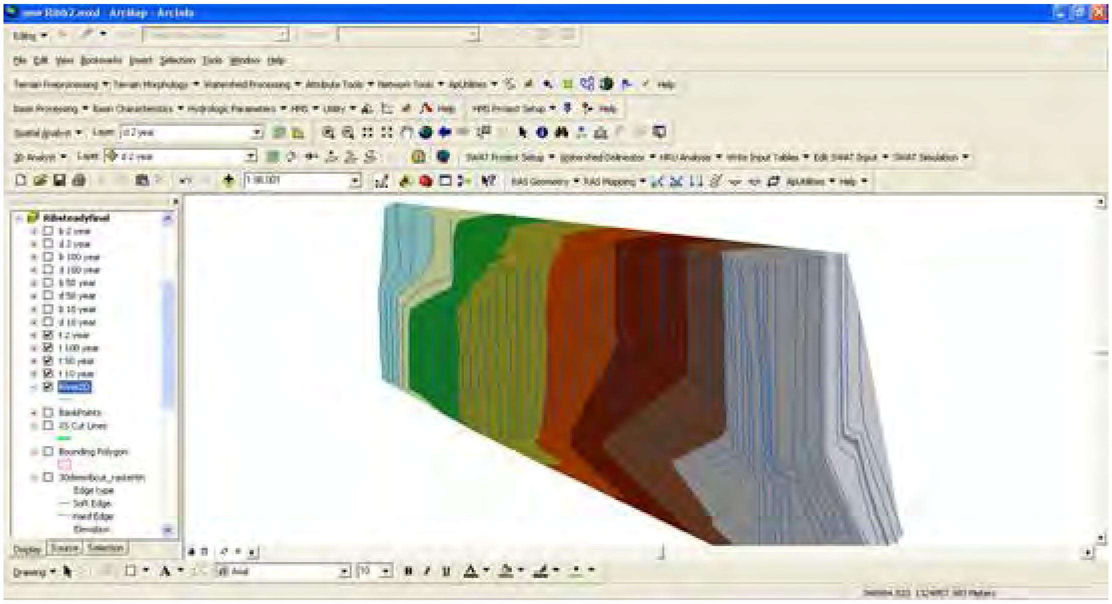

Figure 35: Water surface TIN generated from bounding polygon

ArcGIS with an extension of HEC-GeoRAS then delineates flood plain for different flow conditions. In this paper there are four storm flows considered (2, 10, 50 and 100 year). Flood plain map for each differ in depth, extent and area.

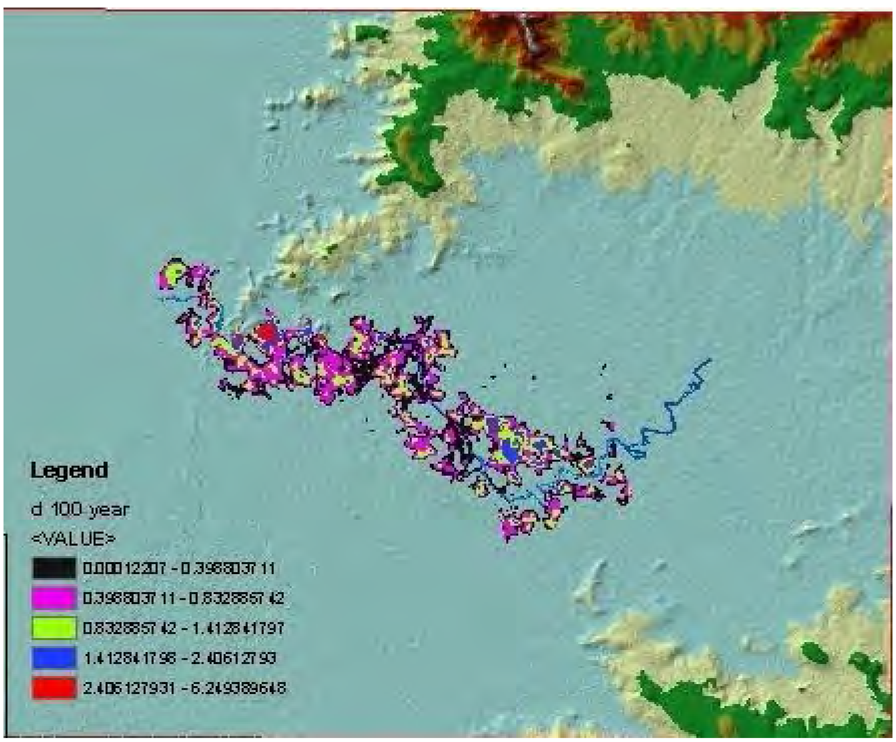

Figure 36: 100 year flood map and depth for the study area

From the above figure for 100 year storm event, it can be seen that the depth of the flood ranges from 0m-6.24m. The flood extent also stretches to about 4km having 2km from each side.

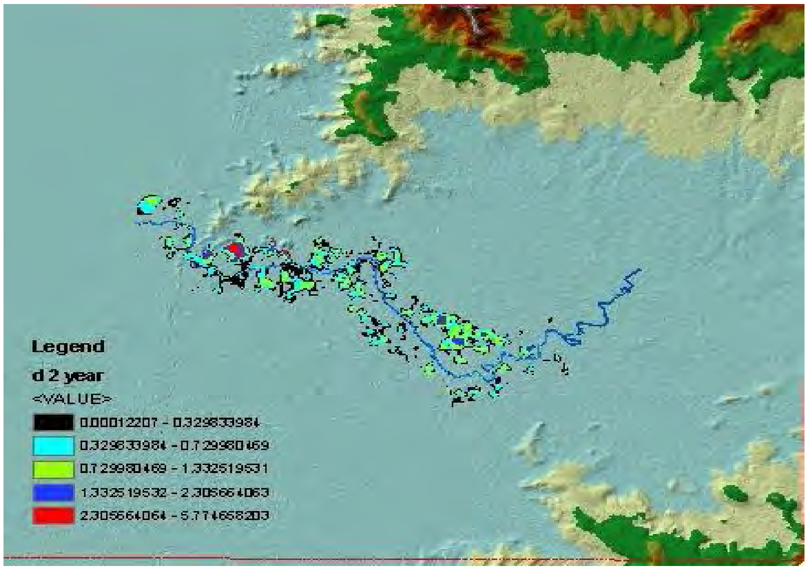

Figure 37: 2 year flow flood inundated areal extent and the corresponding depth

The 2 year flood as shown in the figure above has also a flood depth and extent area. The maximum area inundated is 5.77m which occurred at about 18km from the gage location. Most flooding extents are severing with 100 year and 50 year storm events. This is due to huge amount of the flood flow.

6. RESULT AND DISCUSSION

6.1. Flooding on Libo Kemkem Woreda

Flooding disasters are distributed among different kebele's of Libo Kemkem and Fogera woreda. Most portion of Libo Kemkem suffers high inundation. Kab, Bambiko Tsion and Teza Amba are the villages with high portion of the flood depth and area where as Genda Wuha takes little one.

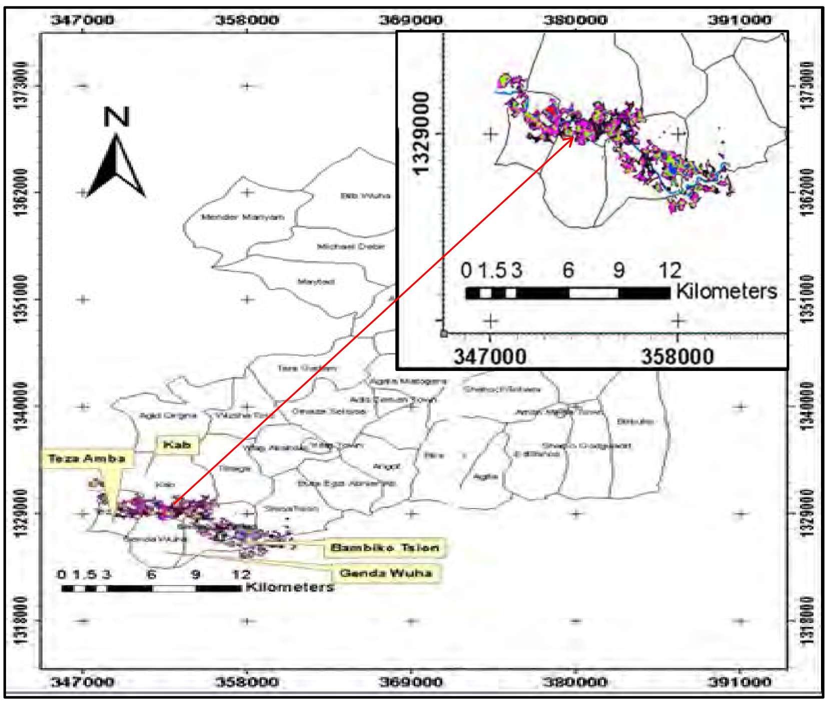

Figure 38: Inundated area of the Libo Kemkem Woreda by 100 year flood

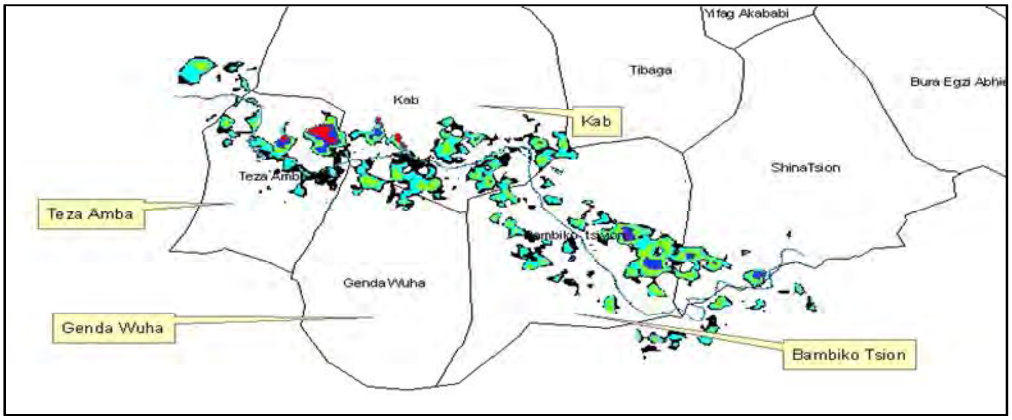

Figure 39: Inundated area of the Libo Kemkem Woreda by 2year year flood

On the other hand, flood depth of less than 0.7m and 0.8m is experienced frequently in the Woreda for 2 year and 100 year flood respectively. This shows that as the magnitude of the flood increases, risk increases with certain proportion.

6.2. Flooding on Fogera Woreda

Unlike to the Libo Kemkem, Fogera Woreda has less risk and vulnerability problems. This is due to the diversion of the Ribb River from Fogera Woreda to the Libo Kemkem by using dyke. The dyke at the intersection avoids the overflow from the new diverted channel to the old channel.

The flooding has also a series effect on Fogera woreda. Even though the Libo Kemkem shares highest proportion, Abua Kokit kebel of the Fogera woreda is highly influenced.

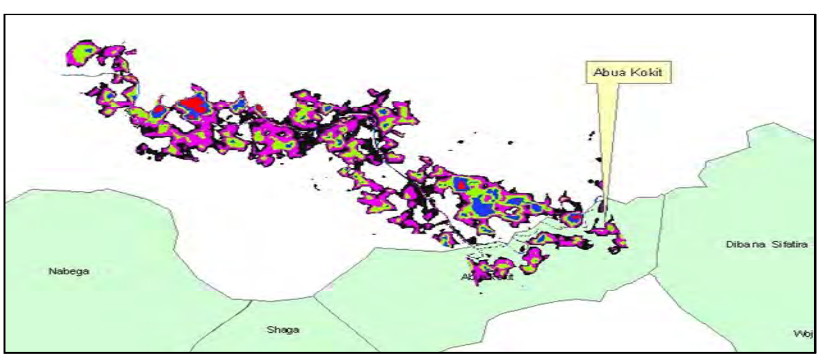

Figure 40: Abua Kokit Kebele of the Fogera Woreda by 100 year flood

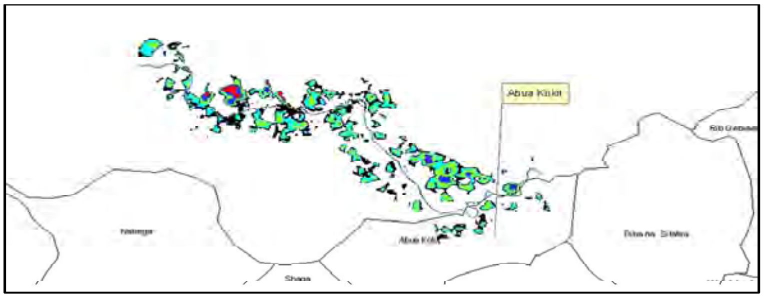

Figure 41: Abua Kokit Kebele of the Fogera Woreda by 2year flood

6.3. Flood Vulnerability Analysis

The vulnerability maps for the flood areas were prepared by intersecting the land use map of the floodplains with the flood area polygon for each of the flood event being modeled.

This depicts the vulnerability aspect of the flood risk in the particular area in terms of the presence or the absence of flooding of a particular return period as a binary model.

Most of the areas around the flood plain are cultivated land with less proportion of agro-pastoral, marsh and pastoral. 88-90% of the flood inundated areas are covered by agricultural land. The remaining 10-12% is covered by agro-pastoral near inlet to Lake Tana.

Most cultivated land of Kab, Teza Amba, Genda Amba, Bambiko Tsion and Abua Kokit are vulnerable by the flood although with varying degree. The first three taking highest proportion of vulnerability.

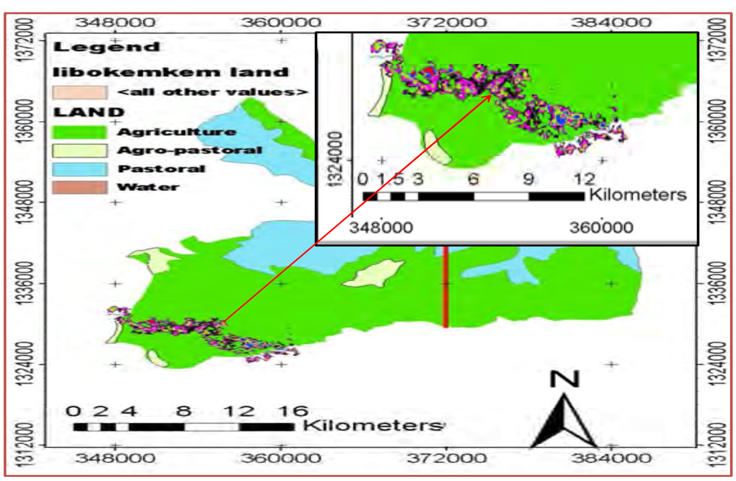

Figure 42: Vulnerability map of the Libo Kemkem and Fogera Woreda by 2 year flood

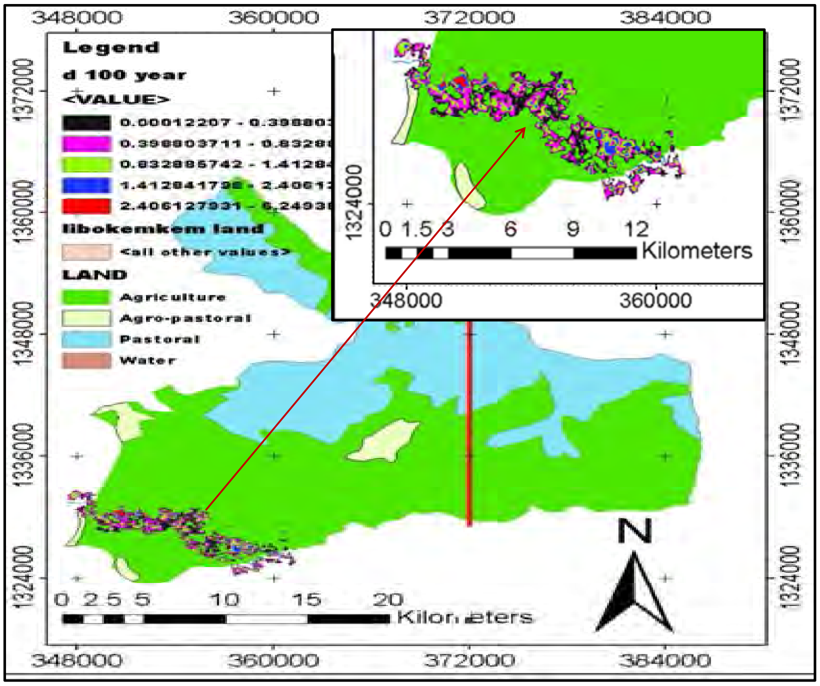

Figure 43: Risk map of the Libo Kemkem and Fogera Woreda by 100 year flood

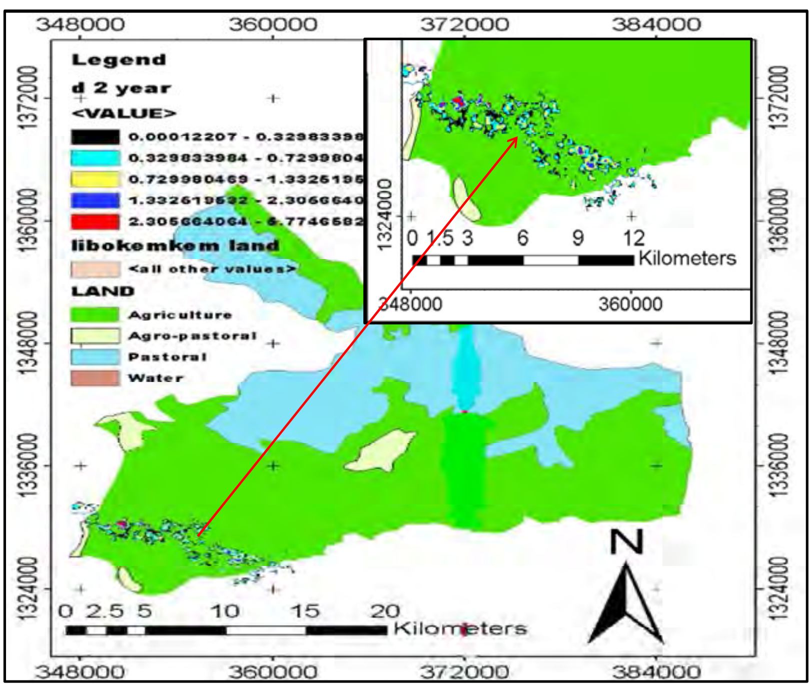

Figure 44: Risk map of the Libo Kemkem and Fogera Woreda by 2 year flood

From the above risk map, most flood depths are in range of 0.4m-0.8m which covers 38% of the total flood extent. The next highest portion is covered by 0m-0.4m which is about 32%. Other flood depths 0.8m-1.4m, 1.4m-2.4m and 2.4-6.2m takes in decreasing proportion.

At about 0.5km-1km in Teza Amba Kebele a high flood depth is observed due to low level of the area. All portion of the area is agricultural land.

	Area inundated (km^2) by a return period of (year)			
Area in	**2**	**10**	**50**	**100**
m^2	12631989	18630676	21311081	22501348
km^2	12.63199	18.63068	21.31108	22.50135

Table13: Inundated area vs. return period

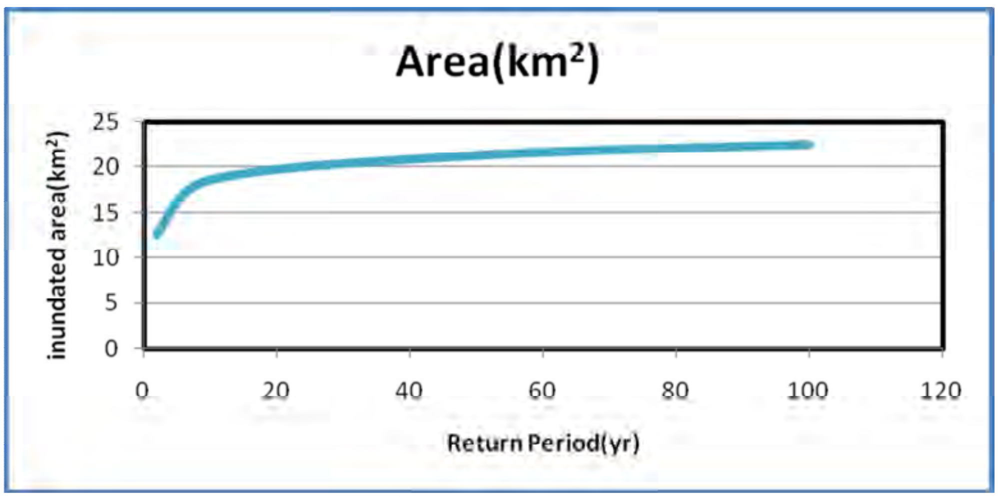

Figure 45: Inundated area (km^2) Vs. Return period

Land use	Depth of flood	% covered	Area (km^2)
Agricultural	0-0.4	32.30	6.4
	0.4-0.8	37.62	7.45
	0.8-1.4	18.08	3.6
	1.4-2.4	9.23	1.8
	2.4-6.2	2.77	0.5
Total		100	**19.8**
Agro-pastoral	0-0.4	23.2	0.55
	0.4-0.8	38.8	0.92
	0.8-1.4	30.5	0.73
	1.4-2.4	3.70	0.088
	2.4-6.2	3.80	0.09
Total		100	**2.385**
River	0-0.4	0	0
	0.4-0.8	57.9	0.18
	0.8-1.4	32.5	0.102
	1.4-2.4	0	0
	2.4-6.2	9.6	0.03
Total		100	**0.315**

Table 14**:** Land use in risk and respective flood depth (100 year flood)

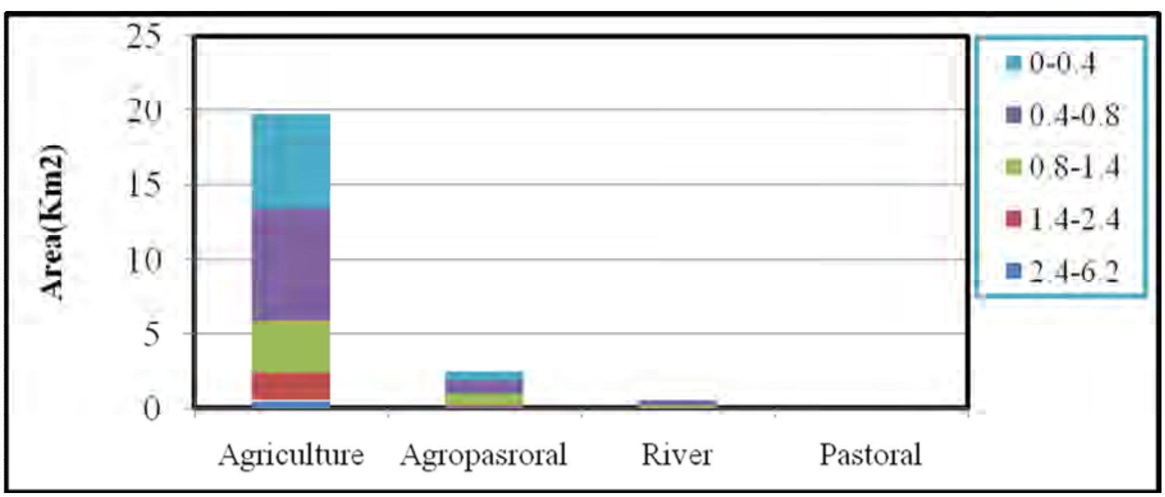

Figure 46: Land use-flood depth-inundated area relationship for 100 year return period flood

The land use area under the influence of modeled flood is summarized in Table and Fig. The figure showed that 88%, 10.6% and 1.4% is covered by agricultural, agro-pastoral and river respectively inundated by 100-year flood having 19.8km^2, 2.385km^2 and 0.315km^2. Similarly, 11.11km^2, 1.34km^2 and 0.177km^2 of agricultural, agro-pastoral and river area are respectively inundated by 2-year flood, which showed flooded area increased with increase in flooding intensity.

6.4. Discussion

The applications of hydraulic model and GIS for floodplain analysis and risk mapping have been limited in countries like Ethiopia, where the availability of the river geometric, topographic and hydrological data are also very limited. The situation of river flooding in Ethiopia is also completely different, as there is much higher variation in the river flows and rivers are completely unregulated.

There are very few flood control structures dykes at river banks and boundary lines which are not clearly defined.

Hence, the floodplain analysis and modeling are subject to number of new sets of constraints. This study presents an approach of conducting a similar study, within these constraints.

- HEC-RAS and ArcGIS were the primary software packages used for this analysis. HEC-GeoRAS extension facilitated the exchange of data between ArcGIS and HEC-RAS.
- Most hydrologic model using HEC-HMS analysis is conducted using personal judgment of parameter estimation. To overcome the gap in result variability, HEC-GeoHMS is a better means.
- The spot elevations from field survey, contour line and good resolution DEM are used to prepare the digital terrain model of the study area so that it can represent the river channel and floodplains adequately.
- The flood discharge of different return period is derived by different method. In this paper the result derived from model result of HEC-HMS is considered representative of the right flow value.
- According to the model results, there is considerable flooding in the area even at flood discharge of 2-year frequency storm. This implies that the channel capacity is small to carry the flood water discharge.

- The flood risk maps prepared indicate a high risk to the agricultural, agro-pastoral land and river with considerable water depth. These areas are the most flood prone areas in the river floodplains and need further considerations for flood protection.

7. CONCLUSION AND RECOMMENDATION

7.1. Conclusion

Flooding around Fogera Woreda causes a considerable damage to life and property. Large coverage of the area with cultivated land makes the problem hard. Past flood forecasting of the area lack the use of modern software.

This study presents a systematic approach in the preparation of flood map of vulnerability and risk with the application of steady flow models and GIS. The major tools/models used in this method is one-dimensional numerical model HEC-RAS and ArcGIS for spatial data processing and HEC-GeoRAS for interfacing between HEC-RAS and ArcGIS.

- The automated floodplain mapping and analysis using these tools provide more efficient, effective and standardized results and saves time and resources.
- The presentation of results in GIS provide a new perspective to the modeled data and this approach can facilitate a transition from a flood hazard model based on the field investigation to a knowledge-based model that can be related to flood intensity.
- The assessment of the vulnerability due to the flooding was made with regard to the land use pattern in the flood areas. The assessment of the flood area indicates that a large percentage (more than 88 %) of vulnerable area lies in flood plain area i.e. agricultural land followed by agro-pastoral and river comprising 10.6% and 1.36% respectively.
- The study also made the assessment of flood hazards with relation to the return period of floods and their water depth. The relationship between the flood area and discharge indicates that there is a medium rate of increase of the flood area with the increase in discharge. The examination of the flood water depth shows that most of the areas under flooding have water depth less than 1.5m with most of the depths range from 0-1.4m.
- Risk map of the study area shows the area under agriculture is highly affected by even the 2-year flood which becomes higher by 100-year storm flood.

- Flooding in Fogera and Libo Kemkem Woreda is devastating even with a 2 year storm. This shows the necessity of construction of engineering structures such as dykes and levees along the river channel and lower part of the flood plain.
- Topographic analysis using GIS and field survey data has a greater efficiency to represent terrain nature exactly. The higher the DEM resolution and enough topographic data, the more accurate the flood map is.
- Hydrologic data are central to flood plain analysis. Availability of hourly time series data increases the model reliability.
- Additional cross sections are used in the areas where the river makes meandering in order to avoid errors during interpolation.

7.2. Recommendations

This study was conducted under major constraint of limited data availability. Therefore, the following recommendations are made for the further studies in the future.

- ***Topographical Data*****:** For modeling flows in overbanks, topographic data should be of high resolution and available enough so that the topography of the floodplains could be properly represented.
- ***Flow data*****:** The major hydrologic parameter, flow data of long time duration is necessary for the calibration and validation of hydrologic model. Unavailability of hourly meteorological data should be addressed.
- ***Use of new technology to generate TIN*****:** TINs obtained using new technologies such as LIDAR (Light Detection and Ranging), which improves the quality of the digital terrain representations is better if used for further study.
- ***Up-to-date DEM*** should be adapted for high accuracy in representation of the study area.
- Since the river morphology of Ribb is changing with time, ***frequent conduction of the channel*** during research work is essential.

REFERENCES

Assefa, K.A., Andel, S.V. and Jonoski, A., 2008, *Flood Forecasting and Early Warning in Lake Tana Sub-basin, Upper Blue Nile, Ethiopia*. Water Mill Working Paper series, no. 16.

Andrysiak, Jr., P.B. (2000), *Visual Floodplain Modeling with Geographic Information Systems*, research of master degree of science in engineering, University of Texas, Austin, USA.

Arcement, G.J. and Schneider, V.R. (1989), *Guide for Selecting Manning's Roughness Coefficients for Natural Channels and Flood Plains*, United States Geological Survey Water supply Paper (WSP 2339).

Beven, K. (2002). *Rainfall-runoff modeling*. Lancaster University, UK.

CFCAS. (2004). *Assessment of Water Resources Risk and Vulnerability to Changing Climatic*. Project Report IV, Calibration, Verification, and Sensitivity Analysis of the HEC-HMS, 23.

Chow, V.T., Maidment, David R. and Mays, L.W. *Applied Hydrology.*New York, 1998.

Cunderlil, J.M. and Simonovic, S.P., 2003, *Assessment of Water Resources Risk and Vulnarebility to Changing Climatic Condition*: *Hydrologic Model Selection for the cfcas project.* Report no. I, the University of Western Ontario, London, Ontario, Canada.

Dhondia, J.F. and Stelling, G.S, 2002, *application of one dimensional-two dimensional integrated hydrologic model for flood simulation and damage assessment*. Proceeding of the Fifth International Conference on Hydroinformatics, Cardiff, 1:265-276.

Dutta D., Herath S., Musiake K., 2000. *Flood inundation simulation in a river basin using a physically based distributed hydrologic mode,*. Hydrological Processes 14 (3), 497–519.

Dyhouse, G., Benn J.R. and Jenifer Hatchet, P.E., 2003, *Flood Plain Modelling Using HEC-RAS*. US Army Corps of Engineers.

Engineers, U. A. (2003). *Geospatial Hydrologic Modeling extension,HEC GeoHMS*, User's Manual. *USACE .Geospatial Hydrologic Modeling Extension HEC-GeoHMS*, U. M. (2003, December). USACE.

Haile, A.T. and Reintijs, T.H.M., 2005, *Effects of LIDAR DEM Resolution in Flood Modeling: A Model Sensitivity Study for the city of Tegucigalpa, Honduras*. MG Vosselman and C.Brenner (Editor), 3:168-173.

HEC-GeoRAS: An extension for support of HEC-RAS using Arcview User's Manual, Version 3.0, U.S. Army Corps of Engineers Hydrologic Engineering Center, Davis, California, April 2000.

Hunter, N.M., Bates, P.D., Horrit, M.S. and Wilson, M.D., 2007, *Simple-spatialy Distributed Models for Predicting Flood Inundation*. A Review Geomorphology, 90:208-225.

Jenson, S.K. and Dominique, J.O. *Extracting Topographic Structure from Digital Elevation Data for Geographic Information Systems Analysis.* Photogrammetric Engineering and Remote Sensing, 54(11), 1593-1600. 1988.

Kafle T.P., Hazarika M. K., Shrestha K.G., Prathumchai K., and Samarakoon L., 2006. *Integration of remote sensing and GIS with flood simulation model for flood hazard mapping in the Bagmati River, Nepal*, Proc. Fifth International Symposium on New Technologies for urban safety of Mega Cities in Asia, Phuket, Thailand.

Masmoudi M., Habaieb H., 1993. *The Performance of Some Realtime Statistical Flood Forecasting Models Seen Through Mmulticriteria Analysis*. Water Resour. Mgmt 7, pp. 57–67.

Merwade, V.M., Maidment, D.R. and Hodges, B.R., 2005, *Geospatial Representation of River Channels.* Jornal of Hydrologic Engineering, 10:243.

Modeling Our World: The ESRI Guide to Geodatabase Design, Arcinfo 8.0, Environmental Systems Research Institute, Inc., California, 1999.

MoWR. (1999). Ministry of Water Resource . *Runoff estimation of Ethiopia river basins.* Nash, J. E. (1970). *River flow forcasting through conceptual models, part one. A discussion of principles. J.Hydrology 10(28)*, 282-290.

Todini E., 1999. *An operational decision support system for flood risk mapping, forecasting and management,* Urban Water 1, 131-143.

UNDP, 1994. *Vulnerability and Risk Assessment*, 2nd Edition, Source: http://www.undmtp.org/english/vulnerability_riskassessment/vulnerability.pdf. pp. 46

USACE, 2003. *Geospatial Hydrologic Modelling Extension HEC-GeoHMS, User's Manual Version 1.1,* US Army Corps of Engineers, Hydrologic Engineering Center, Davis, CA, USA.

ANNEXES

Appendix A: Double Mass Curve of Stations Near Ribb

year	Debretabor	Woreta	Gonder	Bahir dar	Addis zemen	average
1992	3.71	3.1	2.05	3.9	2.94	3.14
1993	4.31	3.9	2.9	4.52	3.5	3.826
1994	4.92	3.6	3.4	4.06	3.04	3.804
1995	4.3	3.6	2.92	4.06	3.04	3.584
1996	4	3.57	2.91	4.04	3.03	3.51
1997	5.5	2.5	3.46	3.31	2	3.354
1998	4.17	4.17	2.97	3.89	1.86	3.412
1999	4.55	4.22	2.99	4.04	3.35	3.83
2000	4.61	3.9	3.26	4.29	4.36	4.084
2001	3.7	3.1	2.95	4.27	1.96	3.196
2002	4.13	3.1	2.67	4.1	3.68	3.536
2003	4.2	3.46	2.25	4.51	3.23	3.53
2004	4.13	3.35	2.75	3.64	3.18	3.41
2005	4.3	3.8	3.18	4.11	3.35	3.748
2006	4.3	4.15	3.26	4.06	3.96	3.946

Table A1: Mean annual precipitation of stations

Debretabor	Woreta	Gonder	Bahir dar	Addis Zemen	cumm aver
3.71	3.1	2.05	3.9	2.94	3.14
8.02	7	4.95	8.42	6.44	6.966
12.94	10.6	8.35	12.48	9.48	10.77
17.24	14.2	11.27	16.54	12.52	14.354
21.24	17.77	14.18	20.58	15.55	17.864
26.74	20.27	17.64	23.89	17.55	21.218
30.91	24.44	20.61	27.78	19.41	24.63
35.46	28.66	23.6	31.82	22.76	28.46
40.07	32.56	26.86	36.11	27.12	32.544
43.77	35.66	29.81	40.38	29.08	35.74
47.9	38.76	32.48	44.48	32.76	39.276
52.1	42.22	34.73	48.99	35.99	42.806
56.23	45.57	37.48	52.63	39.17	46.216
60.53	49.37	40.66	56.74	42.52	49.964
64.83	53.52	43.92	60.8	46.48	53.91

Table A2: Cumulative mean annual of the stations

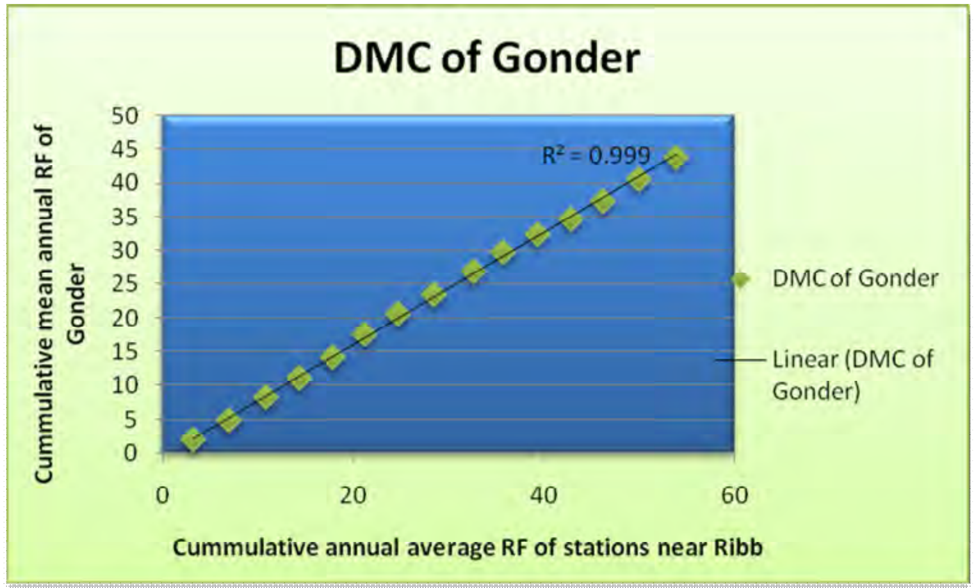

Fig A1: DMC of Gonder

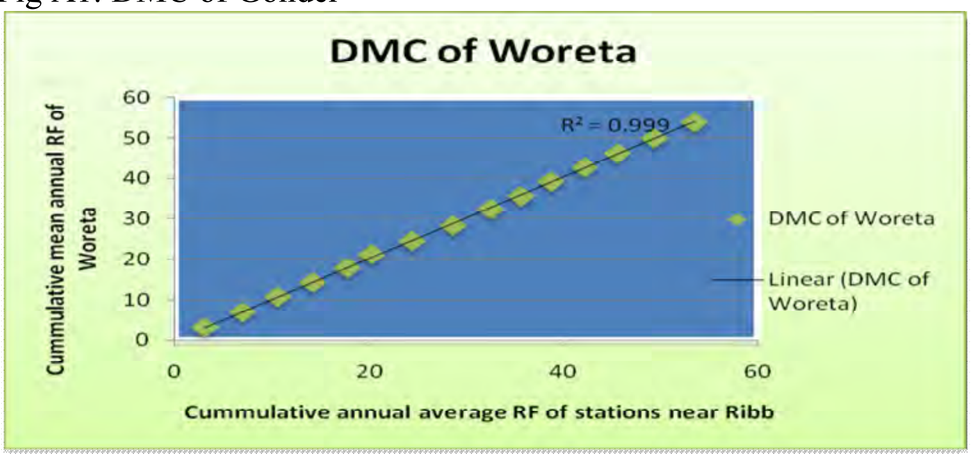

Fig A2: DMC of Woreta

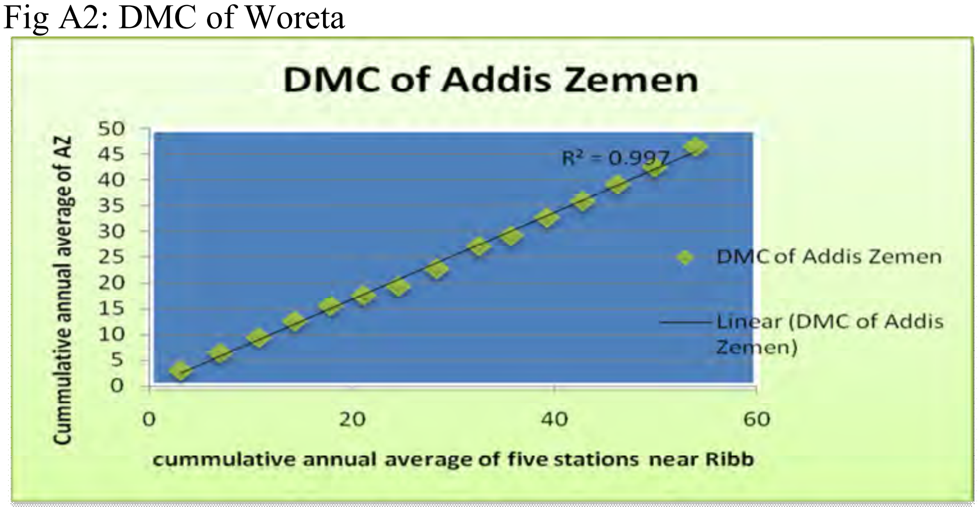

Fig A3: DMC of Addis Zemen

Appendix B: HEC-HMS outputs

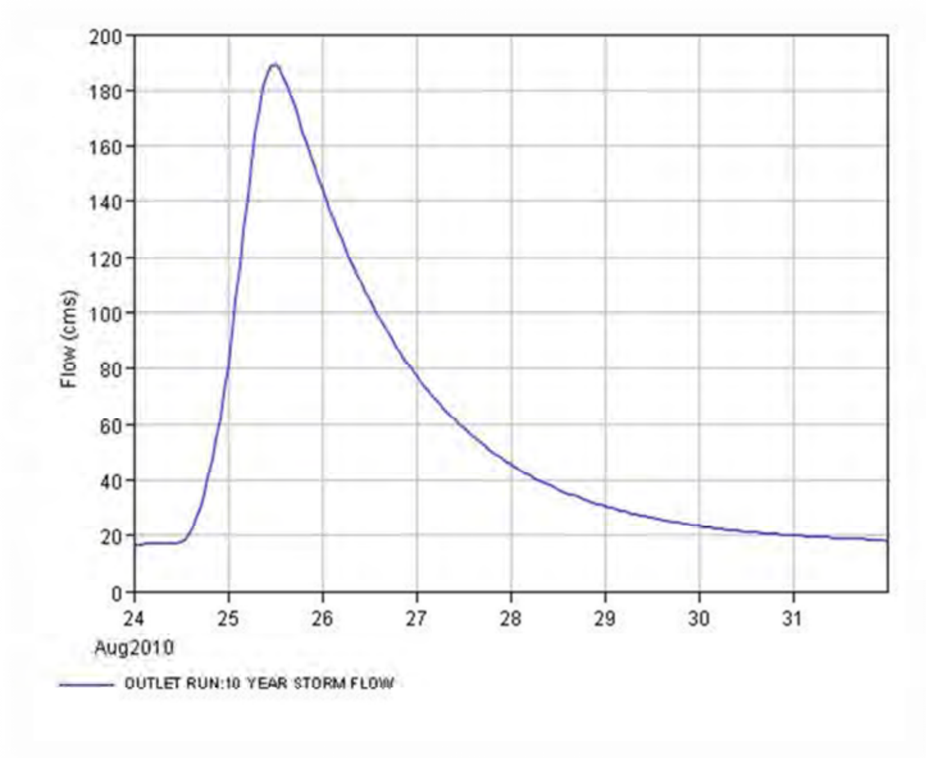

Fig B1: 10 year storm flow hydrograph

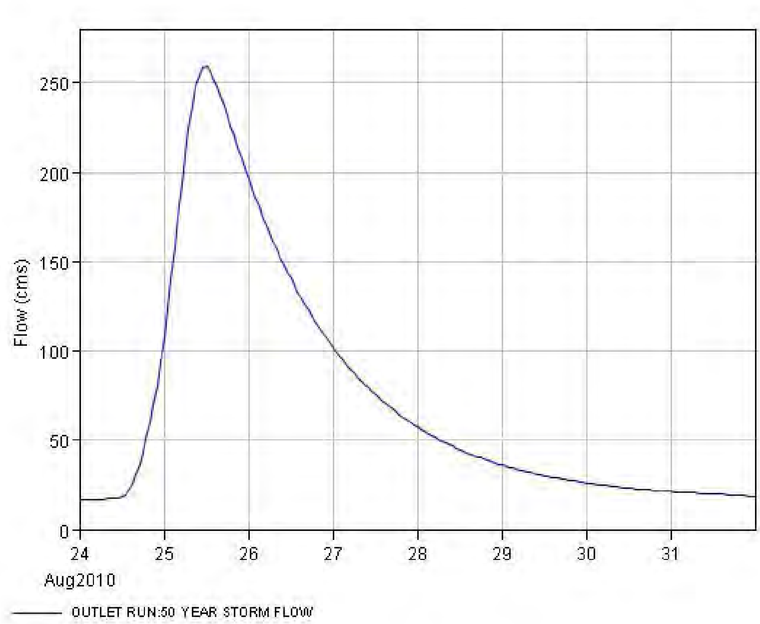

Fig B2: 50 year storm flow hydrograph

Appendix C: HEC-RAS outputs

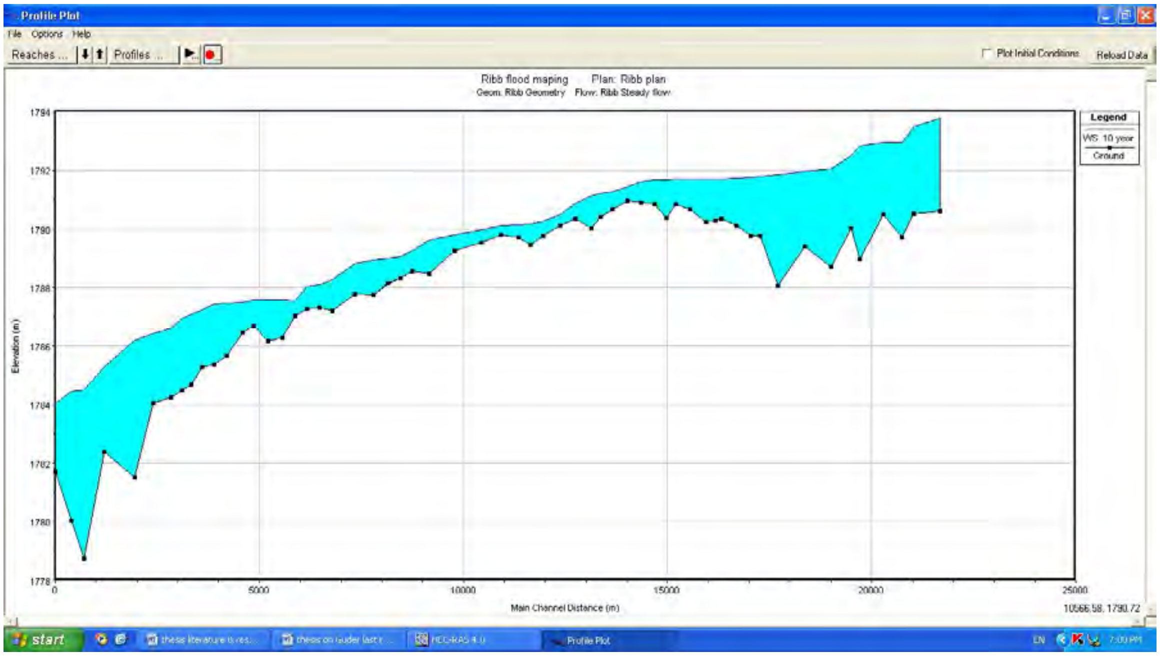

Fig C1: Water Surface Profile of 10 year storm

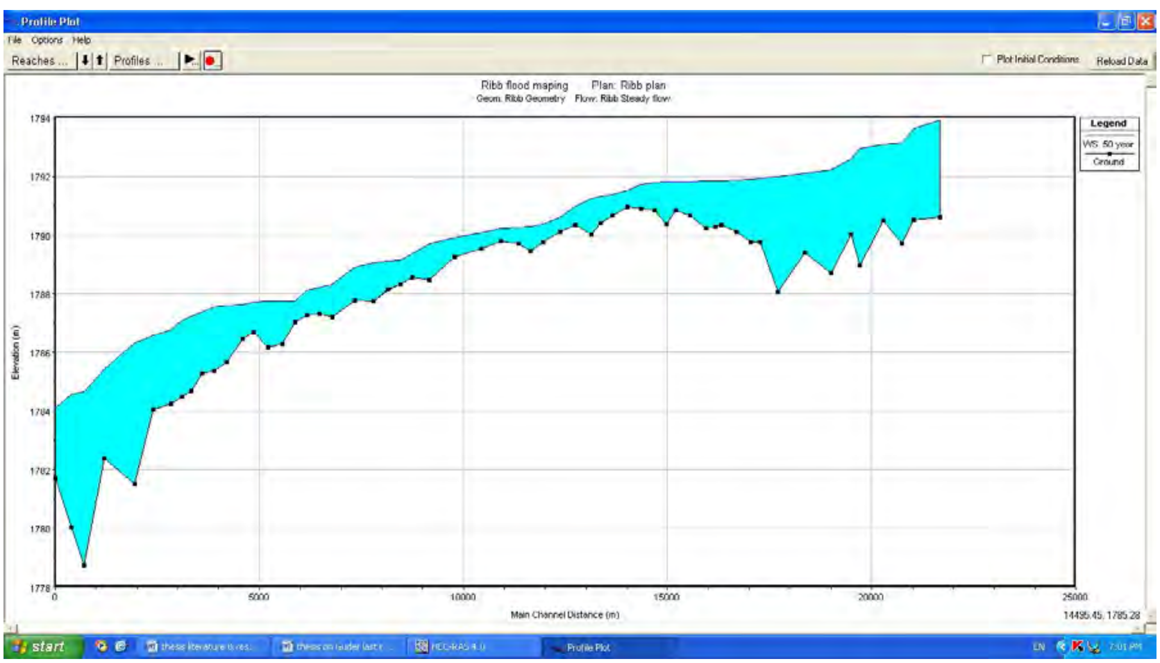

Fig C2: Water Surface Profile of 50 year storm

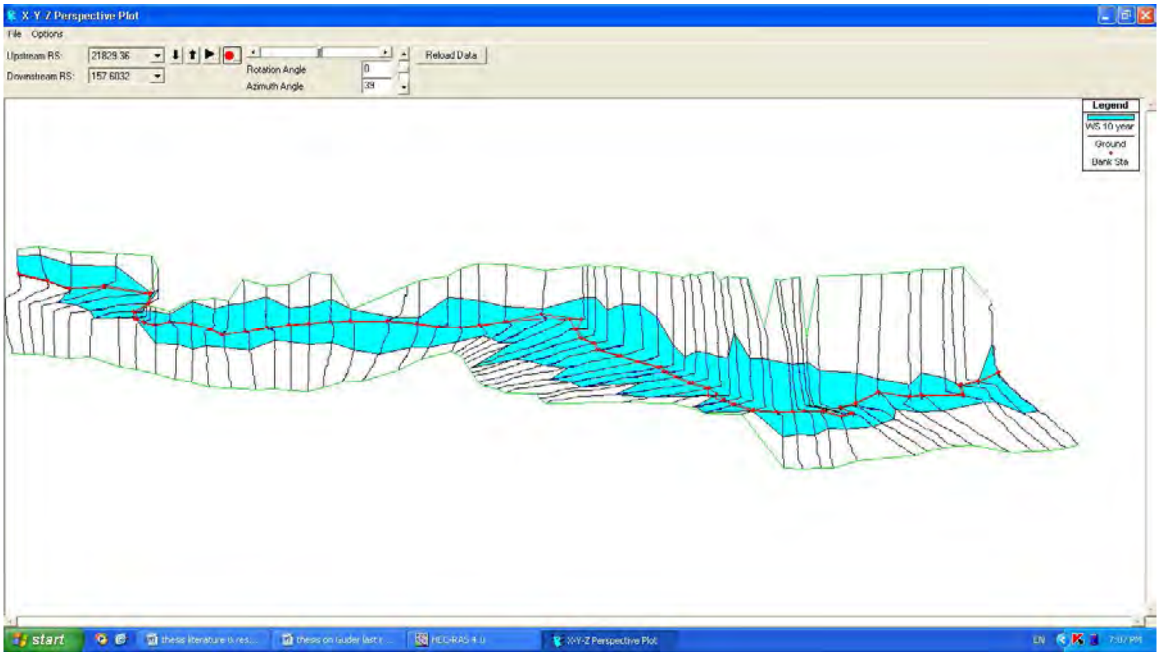

Fig C3: 3D view of 10 year flood

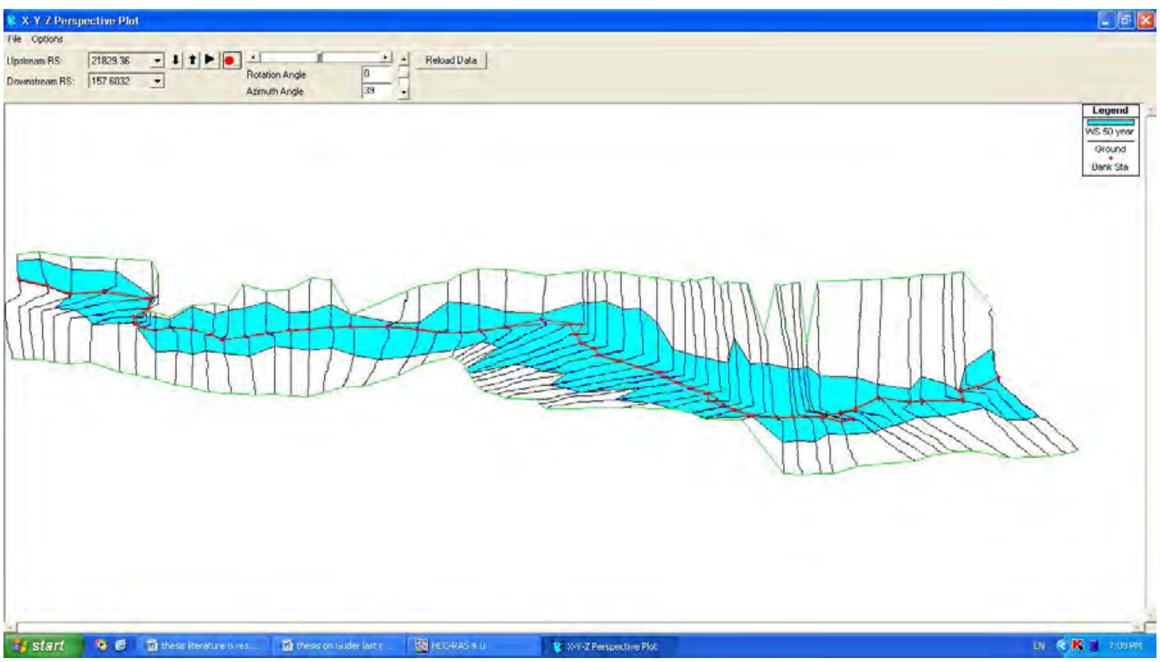

Fig C4: x-y-z perspective view of 50 year flood

Reach	River Sta	Profile	Q Total	Min Ch El	W.S. Elev	Crit W.S.	E.G. Elev	E.G. Slope	Vel Chnl	Flow Area	Top W.
			(m3/s)	(m)	(m)	(m)	(m)	(m/m)	(m/s)	(m2)	(m)
new	21829.36	2 year	91.8	1790.6	1793.38		1793.4	0.0004	0.89	227.3	605.8
new	21829.36	10 year	202.4	1790.6	1793.77		1793.8	0.0004	0.94	566.5	1278
new	21829.36	50 year	273.1	1790.6	1793.9		1793.9	0.0003	0.94	767.6	1620
new	21829.36	100 year	308.4	1790.6	1793.96		1794	0.0003	0.94	866.1	1788
new	21180.82	2 year	91.8	1790.5	1793.11		1793.1	0.0005	0.95	198.1	379.5
new	21180.82	10 year	202.4	1790.5	1793.48		1793.5	0.0006	1.09	391.5	827.6
new	21180.82	50 year	273.1	1790.5	1793.62		1793.6	0.0006	1.15	521.1	1075
new	21180.82	100 year	308.4	1790.5	1793.68		1793.7	0.0006	1.17	586.2	1157
new	20897.08	2 year	91.8	1789.7	1792.24	1791.94	1792.7	0.0067	3.12	29.45	17.71
new	20897.08	10 year	202.4	1789.7	1792.92	1792.92	1793.2	0.0038	2.76	143.8	269.5
new	20897.08	50 year	273.1	1789.7	1793.12		1793.3	0.0033	2.65	212	434.3
new	20897.08	100 year	308.4	1789.7	1793.2		1793.4	0.0031	2.63	247.9	521.3
new	20436.15	2 year	91.8	1790.5	1792.54		1792.5	3E-05	0.2	562.5	534.3
new	20436.15	10 year	202.4	1790.5	1792.94		1792.9	8E-05	0.38	825.9	952.3
new	20436.15	50 year	273.1	1790.5	1793.09		1793.1	0.0001	0.48	987.4	1109
new	20436.15	100 year	308.4	1790.5	1793.15		1793.2	0.0001	0.5	1050	1136
new	19862.43	2 year	91.8	1789	1792.47		1792.5	0.0003	0.87	204.9	531.8
new	19862.43	10 year	202.4	1789	1792.82		1792.9	0.0004	1.1	463.3	971.5
new	19862.43	50 year	273.1	1789	1792.94		1793	0.0005	1.24	587.9	1171
new	19862.43	100 year	308.4	1789	1792.98		1793	0.0005	1.3	643	1265
new	19660.96	2 year	91.8	1790	1791.8	1791.8	1792.3	0.0125	3.09	29.75	30.7
new	19660.96	10 year	202.4	1790	1792.5	1792.5	1792.7	0.0038	2.21	192.8	638.4

new	19660.96	50yr	273.1	1790	1792.58	1792.58	1792.7	0.0043	2.42	243.7	752
new	19660.96	100 year	308.4	1790	1792.63	1792.63	1792.8	0.004	2.38	290.4	911.5
new	19160.75	2 year	91.8	1788.7	1791.71		1791.7	8E-05	0.32	465	684
new	19160.75	10 year	202.4	1788.7	1792.05		1792.1	0.0001	0.43	720.4	797
new	19160.75	50 year	273.1	1788.7	1792.22		1792.2	0.0002	0.48	857.6	878
new	19160.75	100 year	308.4	1788.7	1792.28		1792.3	0.0002	0.51	915	930.1
new	18515.08	2 year	91.8	1789.4	1791.63		1791.6	0.0002	0.49	369.5	783.6
new	18515.08	10 year	202.4	1789.4	1791.95		1792	0.0002	0.57	678.8	1216
new	18515.08	50 year	273.1	1789.4	1792.09		1792.1	0.0003	0.65	884.1	1502
new	18515.08	100 year	308.4	1789.4	1792.15		1792.2	0.0003	0.65	976.1	1541
new	17866.96	2 year	91.8	1788.1	1791.53		1791.5	0.0001	0.43	507.1	1173
new	17866.96	10 year	202.4	1788.1	1791.85		1791.9	0.0001	0.46	953.2	1559
new	17866.96	50 year	273.1	1788.1	1791.98		1792	0.0001	0.48	1177	1680
new	17866.96	100 year	308.4	1788.1	1792.04		1792.1	0.0001	0.49	1278	1733
new	17427.57	2 year	91.8	1789.8	1791.46		1791.5	0.0002	0.39	466.8	1389
new	17427.57	10 year	202.4	1789.8	1791.79		1791.8	0.0001	0.33	1002	1822
new	17427.57	50 year	273.1	1789.8	1791.93		1791.9	0.0001	0.33	1267	1990
new	17427.57	100 year	308.4	1789.8	1791.99		1792	0.0001	0.33	1388	2058
new	17186.57	2 year	91.8	1789.8	1791.41		1791.4	0.0002	0.37	410.9	981.9
new	17186.57	10 year	202.4	1789.8	1791.76		1791.8	0.0002	0.36	810.6	1302
new	17186.57	50 year	273.1	1789.8	1791.9		1791.9	0.0002	0.39	1007	1511
new	17186.57	100 year	308.4	1789.8	1791.96		1792	0.0002	0.4	1099	1577
new	16834.67	2 year	91.8	1790.1	1791.37		1791.4	6E-05	0.21	631.6	1138
new	16834.67	10 year	202.4	1790.1	1791.73		1791.7	7E-05	0.27	1086	1424

new	16834.67	50 yr	273.1	1790.1	1791.86		1791.9	9E-05	0.31	1284	1503
new	16834.67	100 year	308.4	1790.1	1791.92		1791.9	9E-05	0.33	1374	1567
new	16482.41	2 year	91.8	1790.3	1791.36		1791.4	3E-05	0.1	940.7	1605
new	16482.41	10 year	202.4	1790.3	1791.71		1791.7	3E-05	0.14	1561	1940
new	16482.41	50 year	273.1	1790.3	1791.84		1791.8	4E-05	0.17	1823	2037
new	16482.41	100 year	308.4	1790.3	1791.9		1791.9	4E-05	0.18	1944	2137
new	16324.36	2 year	91.8	1790.3	1791.36		1791.4	2E-05	0.09	977.5	1480
new	16324.36	10 year	202.4	1790.3	1791.7		1791.7	3E-05	0.12	1543	1842
new	16324.36	50 year	273.1	1790.3	1791.84		1791.8	4E-05	0.14	1794	1973
new	16324.36	100 year	308.4	1790.3	1791.89		1791.9	4E-05	0.15	1909	2098
new	16105.07	2 year	91.8	1790.2	1791.35		1791.4	7E-06	0.05	1593	2050
new	16105.07	10 year	202.4	1790.2	1791.7		1791.7	1E-05	0.08	2405	2564
new	16105.07	50 year	273.1	1790.2	1791.83		1791.8	1E-05	0.09	2752	2764
new	16105.07	100 year	308.4	1790.2	1791.89		1791.9	2E-05	0.1	2911	2830
new	15715.24	2 year	91.8	1790.7	1791.35		1791.4	1E-05	0.05	1177	1443
new	15715.24	10 year	202.4	1790.7	1791.7		1791.7	2E-05	0.08	1725	1864
new	15715.24	50 year	273.1	1790.7	1791.82		1791.8	3E-05	0.1	1978	2131
new	15715.24	100 year	308.4	1790.7	1791.88		1791.9	3E-05	0.12	2099	2214
new	15352.89	2 year	91.8	1790.8	1791.34		1791.3	4E-05	0.07	919.6	1808
new	15352.89	10 year	202.4	1790.8	1791.69		1791.7	4E-05	0.1	1597	2085
new	15352.89	50 year	273.1	1790.8	1791.81		1791.8	4E-05	0.11	1866	2155
new	15352.89	100 year	308.4	1790.8	1791.87		1791.9	4E-05	0.12	1981	2185
new	15119.36	2 year	91.8	1790.4	1791.34		1791.3	5E-06	0.05	1389	1411
new	15119.36	10 year	202.4	1790.4	1791.68		1791.7	2E-05	0.09	1988	2120

new	15119.36	50 yr	273.1	1790.4	1791.81		1791.8	2E-05	0.12	2272	2372
new	15119.36	100 year	308.4	1790.4	1791.86		1791.9	2E-05	0.13	2399	2429
new	14842.13	2 year	91.8	1790.8	1791.34		1791.3	2E-05	0.06	732	744.1
new	14842.13	10 year	202.4	1790.8	1791.67		1791.7	5E-05	0.12	1021	1003
new	14842.13	50 year	273.1	1790.8	1791.79		1791.8	6E-05	0.13	1149	1106
new	14842.13	100 year	308.4	1790.8	1791.85		1791.9	7E-05	0.12	1208	1187
new	14516.11	2 year	91.8	1790.9	1791.31		1791.3	0.0005	0.27	242.8	502.6
new	14516.11	10 year	202.4	1790.9	1791.62		1791.6	0.0006	0.45	461.4	890.4
new	14516.11	50 year	273.1	1790.9	1791.73		1791.8	0.0007	0.52	570	1107
new	14516.11	100 year	308.4	1790.9	1791.78		1791.8	0.0007	0.55	621.6	1177
new	14167.52	2 year	91.8	1790.9	1791.15		1791.2	0.0004	0.16	281.4	699.5
new	14167.52	10 year	202.4	1790.9	1791.43		1791.4	0.0006	0.33	577.2	1508
new	14167.52	50 year	273.1	1790.9	1791.54		1791.5	0.0005	0.35	752.6	1662
new	14167.52	100 year	308.4	1790.9	1791.58		1791.6	0.0005	0.37	827.6	1716
new	13803.91	2 year	91.8	1790.7	1791.03		1791	0.0003	0.17	396.3	990.9
new	13803.91	10 year	202.4	1790.7	1791.28		1791.3	0.0003	0.28	682.5	1340
new	13803.91	50 year	273.1	1790.7	1791.39		1791.4	0.0003	0.32	851.4	1586
new	13803.91	100 year	308.4	1790.7	1791.43		1791.4	0.0003	0.34	920.2	1624
new	13512.28	2 year	91.8	1790.4	1790.97		1791	0.0002	0.18	458.3	987.2
new	13512.28	10 year	202.4	1790.4	1791.2		1791.2	0.0002	0.26	776.6	1597
new	13512.28	50 year	273.1	1790.4	1791.31		1791.3	0.0002	0.3	973.5	1977
new	13512.28	100 year	308.4	1790.4	1791.35		1791.4	0.0002	0.32	1054	2074
new	13288.03	2 year	91.8	1790	1790.9		1790.9	0.0008	0.48	284.7	995
new	13288.03	10 year	202.4	1790	1791.12		1791.1	0.0007	0.56	562.4	1511

new	13288.03	50 yr	273.1	1790	1791.23		1791.2	0.0006	0.59	761.9	1937
new	13288.03	100 year	308.4	1790	1791.27		1791.3	0.0006	0.6	836.4	1974
new	12896.89	2 year	91.8	1790.4	1790.65		1790.7	0.0006	0.19	286.1	824.7
new	12896.89	10 year	202.4	1790.4	1790.86		1790.9	0.0007	0.29	496.1	1152
new	12896.89	50 year	273.1	1790.4	1790.98		1791	0.0007	0.34	651.3	1425
new	12896.89	100 year	308.4	1790.4	1791.02		1791	0.0007	0.36	705.1	1470
new	12528.02	2 year	91.8	1790.1	1790.29		1790.3	0.002	0.25	195.7	733.5
new	12528.02	10 year	202.4	1790.1	1790.49		1790.5	0.0016	0.4	363.7	969.4
new	12528.02	50 year	273.1	1790.1	1790.59		1790.6	0.0017	0.46	472.7	1139
new	12528.02	100 year	308.4	1790.1	1790.63		1790.7	0.0016	0.47	522.3	1166
new	12110.01	2 year	91.8	1789.8	1790.03		1790	0.0003	0.15	424.1	1353
new	12110.01	10 year	202.4	1789.8	1790.27		1790.3	0.0003	0.25	805.8	1708
new	12110.01	50 year	273.1	1789.8	1790.38		1790.4	0.0003	0.29	997.9	1786
new	12110.01	100 year	308.4	1789.8	1790.43		1790.4	0.0003	0.3	1086	1851
new	11797.6	2 year	91.8	1789.5	1789.92		1789.9	0.0004	0.22	372.5	1158
new	11797.6	10 year	202.4	1789.5	1790.18		1790.2	0.0003	0.28	788.9	1866
new	11797.6	50 year	273.1	1789.5	1790.3		1790.3	0.0003	0.31	1017	2104
new	11797.6	100 year	308.4	1789.5	1790.35		1790.4	0.0003	0.33	1124	2290
new	11505.25	2 year	91.8	1789.7	1789.9		1789.9	3E-05	0.03	931.6	1622
new	11505.25	10 year	202.4	1789.7	1790.16		1790.2	5E-05	0.09	1432	2226
new	11505.25	50 year	273.1	1789.7	1790.27		1790.3	6E-05	0.12	1700	2552
new	11505.25	100 year	308.4	1789.7	1790.32		1790.3	6E-05	0.13	1825	2696
new	11067.91	2 year	91.8	1789.8	1789.88		1789.9	0.0001	0.04	589.9	1544
new	11067.91	10 year	202.4	1789.8	1790.12		1790.1	0.0001	0.1	1062	2131

new	11067.91	50 yr	273.1	1789.8	1790.23		1790.2	0.0001	0.13	1310	2420
new	11067.91	100 year	308.4	1789.8	1790.28		1790.3	0.0001	0.14	1422	2519
new	10591.12	2 year	91.8	1789.5	1789.74		1789.8	0.0024	0.45	194.6	939.8
new	10591.12	10 year	202.4	1789.5	1789.98		1790	0.0011	0.47	491.7	1458
new	10591.12	50 year	273.1	1789.5	1790.09		1790.1	0.0009	0.31	677.5	1999
new	10591.12	100 year	308.4	1789.5	1790.14		1790.1	0.0008	0.29	781.3	2230
new	9932.791	2 year	91.8	1789.2	1789.56		1789.6	0.0001	0.13	484.6	1196
new	9932.791	10 year	202.4	1789.2	1789.8		1789.8	0.0002	0.12	817.1	1488
new	9932.791	50 year	273.1	1789.2	1789.91		1789.9	0.0002	0.17	979.6	1574
new	9932.791	100 year	308.4	1789.2	1789.96		1790	0.0002	0.19	1054	1638
new	9318.204	2 year	91.8	1788.5	1789.4		1789.4	0.0009	0.44	270.6	931.6
new	9318.204	10 year	202.4	1788.5	1789.62		1789.6	0.0007	0.53	514.3	1340
new	9318.204	50 year	273.1	1788.5	1789.71		1789.7	0.0007	0.57	645.6	1397
new	9318.204	100 year	308.4	1788.5	1789.75		1789.8	0.0007	0.6	698.6	1422
new	8898.782	2 year	91.8	1788.6	1789.03		1789	0.0009	0.37	243.2	718.2
new	8898.782	10 year	202.4	1788.6	1789.26		1789.3	0.0011	0.56	450.1	1240
new	8898.782	50 year	273.1	1788.6	1789.36		1789.4	0.001	0.62	601.4	1569
new	8898.782	100 year	308.4	1788.6	1789.4		1789.4	0.001	0.64	660.6	1623
new	8620.744	2 year	91.8	1788.3	1788.79		1788.8	0.0008	0.41	256.8	923
new	8620.744	10 year	202.4	1788.3	1789.04		1789	0.0006	0.48	566.5	1626
new	8620.744	50 year	273.1	1788.3	1789.15		1789.2	0.0006	0.53	759.4	1921
new	8620.744	100 year	308.4	1788.3	1789.19		1789.2	0.0006	0.54	850.7	2040
new	8305.458	2 year	91.8	1788.1	1788.77		1788.8	4E-05	0.08	940.9	1828
new	8305.458	10 year	202.4	1788.1	1789		1789	6E-05	0.14	1413	2297

new	8305.458	50 yr	273.1	1788.1	1789.1		1789.1	7E-05	0.16	1661	2421
new	8305.458	100 year	308.4	1788.1	1789.15		1789.2	7E-05	0.18	1769	2467
new	7960.104	2 year	91.8	1787.8	1788.74		1788.7	0.0003	0.42	344.4	942.8
new	7960.104	10 year	202.4	1787.8	1788.95		1789	0.0004	0.57	581.5	1220
new	7960.104	50 year	273.1	1787.8	1789.05		1789.1	0.0004	0.63	705.2	1302
new	7960.104	100 year	308.4	1787.8	1789.09		1789.1	0.0005	0.65	759	1346
new	7498.107	2 year	91.8	1787.8	1788.62		1788.6	0.0002	0.24	506.3	1568
new	7498.107	10 year	202.4	1787.8	1788.81		1788.8	0.0003	0.33	811.2	1693
new	7498.107	50 year	273.1	1787.8	1788.9		1788.9	0.0003	0.37	967.2	1715
new	7498.107	100 year	308.4	1787.8	1788.93		1788.9	0.0003	0.39	1025	1720
new	6930.722	2 year	91.8	1787.2	1788.17	1788.17	1788.3	0.0156	2.12	88.28	517.9
new	6930.722	10 year	202.4	1787.2	1788.28	1788.28	1788.4	0.0163	2.41	156.1	728.1
new	6930.722	50 year	273.1	1787.2	1788.32	1788.32	1788.5	0.0183	2.65	190.1	870.6
new	6930.722	100 year	308.4	1787.2	1788.37	1788.37	1788.5	0.0161	2.61	241.8	1256
new	6631.115	2 year	91.8	1787.3	1787.89		1787.9	4E-05	0.09	657.5	913.3
new	6631.115	10 year	202.4	1787.3	1788.11		1788.1	1E-04	0.18	879	1078
new	6631.115	50 year	273.1	1787.3	1788.2		1788.2	0.0001	0.23	981.4	1184
new	6631.115	100 year	308.4	1787.3	1788.25		1788.3	0.0001	0.25	1040	1253
new	6321.055	2 year	91.8	1787.3	1787.85	1787.45	1787.9	0.0004	0.3	361.1	1016
new	6321.055	10 year	202.4	1787.3	1788.05		1788.1	0.0005	0.4	580.3	1161
new	6321.055	50 year	273.1	1787.3	1788.12		1788.1	0.0006	0.46	664	1201
new	6321.055	100 year	308.4	1787.3	1788.16		1788.2	0.0006	0.48	714	1293
new	6029.344	2 year	91.8	1787	1787.4	1787.4	1787.5	0.0261	1.96	71.76	427.2
new	6029.344	10 year	202.4	1787	1787.55	1787.53	1787.6	0.0162	1.78	157.8	836.6

new	6029.344	50 yr	273.1	1787	1787.74		1787.8	0.0039	1.11	350.9	1075
new	6029.344	100 year	308.4	1787	1787.82		1787.9	0.0026	0.96	435.5	1149
new	5710.898	2 year	91.8	1786.3	1787.25		1787.3	6E-06	0.05	1445	1669
new	5710.898	10 year	202.4	1786.3	1787.6		1787.6	1E-05	0.09	2104	2004
new	5710.898	50 year	273.1	1786.3	1787.75		1787.8	1E-05	0.11	2419	2071
new	5710.898	100 year	308.4	1786.3	1787.82		1787.8	2E-05	0.12	2569	2141
new	5365.28	2 year	91.8	1786.2	1787.24		1787.3	2E-06	0.03	1628	1223
new	5365.28	10 year	202.4	1786.2	1787.59		1787.6	6E-06	0.07	2100	1488
new	5365.28	50 year	273.1	1786.2	1787.75		1787.8	9E-06	0.09	2343	1672
new	5365.28	100 year	308.4	1786.2	1787.82		1787.8	1E-05	0.1	2464	1738
new	5013.05	2 year	91.8	1786.7	1787.24		1787.2	4E-05	0.11	534.3	635.5
new	5013.05	10 year	202.4	1786.7	1787.59		1787.6	9E-05	0.23	886.8	1339
new	5013.05	50 year	273.1	1786.7	1787.74		1787.7	0.0001	0.3	1112	1633
new	5013.05	100 year	308.4	1786.7	1787.81		1787.8	0.0001	0.34	1230	1715
new	4750.999	2 year	91.8	1786.5	1787.16		1787.2	0.0075	1.57	105.2	439
new	4750.999	10 year	202.4	1786.5	1787.5		1787.5	0.0022	1.19	294.9	724.2
new	4750.999	50 year	273.1	1786.5	1787.64		1787.7	0.0019	1.23	415	980.9
new	4750.999	100 year	308.4	1786.5	1787.7		1787.7	0.0017	1.2	476.9	1039
new	4357.081	2 year	91.8	1785.6	1787.17		1787.2	1E-05	0.1	972.8	1159
new	4357.081	10 year	202.4	1785.6	1787.48		1787.5	3E-05	0.17	1359	1340
new	4357.081	50 year	273.1	1785.6	1787.61		1787.6	4E-05	0.21	1553	1577
new	4357.081	100 year	308.4	1785.6	1787.67		1787.7	4E-05	0.22	1646	1678
new	4046.409	2 year	91.8	1785.4	1787.12		1787.2	0.0012	1.15	175.7	543.5
new	4046.409	10 year	202.4	1785.4	1787.43		1787.5	0.0008	1.11	403.7	922.8

new	4046.409	50 yr	273.1	1785.4	1787.56		1787.6	0.0008	1.12	537.1	1115
new	4046.409	100 year	308.4	1785.4	1787.62		1787.6	0.0007	1.12	600.7	1178
new	3764.391	2 year	91.8	1785.3	1786.93		1786.9	0.0005	0.64	241.6	466.7
new	3764.391	10 year	202.4	1785.3	1787.25		1787.3	0.0006	0.79	443.2	883
new	3764.391	50 year	273.1	1785.3	1787.4		1787.4	0.0005	0.81	605.1	1261
new	3764.391	100 year	308.4	1785.3	1787.46		1787.5	0.0005	0.81	687.1	1336
new	3490.179	2 year	91.8	1784.7	1786.8		1786.8	0.0005	0.88	235.3	503.2
new	3490.179	10 year	202.4	1784.7	1787.1		1787.1	0.0006	1.03	404.9	610.3
new	3490.179	50 year	273.1	1784.7	1787.25		1787.3	0.0006	1.07	500.3	649.5
new	3490.179	100 year	308.4	1784.7	1787.32		1787.3	0.0006	1.1	542.8	655.5
new	3267.181	2 year	91.8	1784.5	1786.66		1786.7	0.0006	0.92	200.9	410
new	3267.181	10 year	202.4	1784.5	1786.94		1787	0.0008	1.19	315.4	420.7
new	3267.181	50 year	273.1	1784.5	1787.08		1787.1	0.0009	1.3	376	426.2
new	3267.181	100 year	308.4	1784.5	1787.14		1787.2	0.0009	1.35	401.6	428.5
new	2991.166	2 year	91.8	1784.2	1786.2		1786.3	0.0037	1.79	79.82	326.4
new	2991.166	10 year	202.4	1784.2	1786.62		1786.7	0.0016	1.42	269	530.8
new	2991.166	50 year	273.1	1784.2	1786.78		1786.8	0.0014	1.41	363.2	758.6
new	2991.166	100 year	308.4	1784.2	1786.84		1786.9	0.0013	1.42	413.3	855.8
new	2559.985	2 year	91.8	1784	1786.04		1786	0.0002	0.53	314.6	618.6
new	2559.985	10 year	202.4	1784	1786.44		1786.5	0.0002	0.61	622.1	932
new	2559.985	50 year	273.1	1784	1786.59		1786.6	0.0003	0.68	771.6	1125
new	2559.985	100 year	308.4	1784	1786.64		1786.7	0.0003	0.71	837.4	1154
new	2097.512	2 year	91.8	1781.5	1785.84		1785.9	0.0005	1.12	153.4	282.8
new	2097.512	10 year	202.4	1781.5	1786.21		1786.3	0.0008	1.53	309.7	577.9

new	2097.512	50 yr	273.1	1781.5	1786.31		1786.4	0.001	1.75	373.4	670.1
new	2097.512	100 year	308.4	1781.5	1786.35		1786.4	0.0011	1.85	400.4	694
new	1361.816	2 year	91.8	1782.4	1784.99	1784.99	1785.1	0.0035	2.08	92.51	396.1
new	1361.816	10 year	202.4	1782.4	1785.29		1785.4	0.0023	1.81	288.9	1031
new	1361.816	50 year	273.1	1782.4	1785.44		1785.5	0.0016	1.57	467.4	1390
new	1361.816	100 year	308.4	1782.4	1785.49		1785.5	0.0014	1.49	540.1	1460
new	855.9996	2 year	91.8	1778.8	1784.2		1784.3	0.0006	1.22	150.2	275.8
new	855.9996	10 year	202.4	1778.8	1784.51		1784.6	0.0011	1.69	245.8	335
new	855.9996	50 year	273.1	1778.8	1784.66		1784.7	0.0013	1.89	298.7	376.6
new	855.9996	100 year	308.4	1778.8	1784.72		1784.8	0.0014	1.97	323	392.5
new	540.4757	2 year	91.8	1780	1784.16		1784.2	0.0001	0.48	427.3	719.8
new	540.4757	10 year	202.4	1780	1784.44		1784.4	0.0002	0.64	641	804.7
new	540.4757	50 year	273.1	1780	1784.57		1784.6	0.0002	0.72	750.6	844.7
new	540.4757	100 year	308.4	1780	1784.62		1784.6	0.0002	0.75	797.5	864
new	157.6032	2 year	91.8	1781.7	1783.9	1783.9	1784	0.0051	2.13	96.71	348.6
new	157.6032	10 year	202.4	1781.7	1784.06	1784.06	1784.2	0.0077	2.73	160.1	439.3
new	157.6032	50 year	273.1	1781.7	1784.11	1784.11	1784.3	0.0098	3.12	183.3	454.6
new	157.6032	100 year	308.4	1781.7	1784.15	1784.15	1784.3	0.0097	3.14	201.2	465.6

Table C1: Output table of HEC-RAS

Appendix D: Flood Map Results

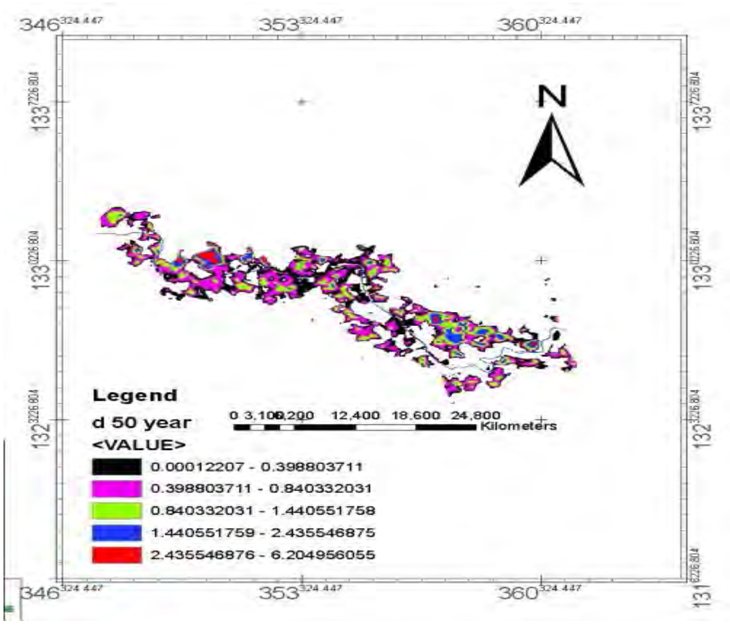

Fig D1**:** 50 year flood map

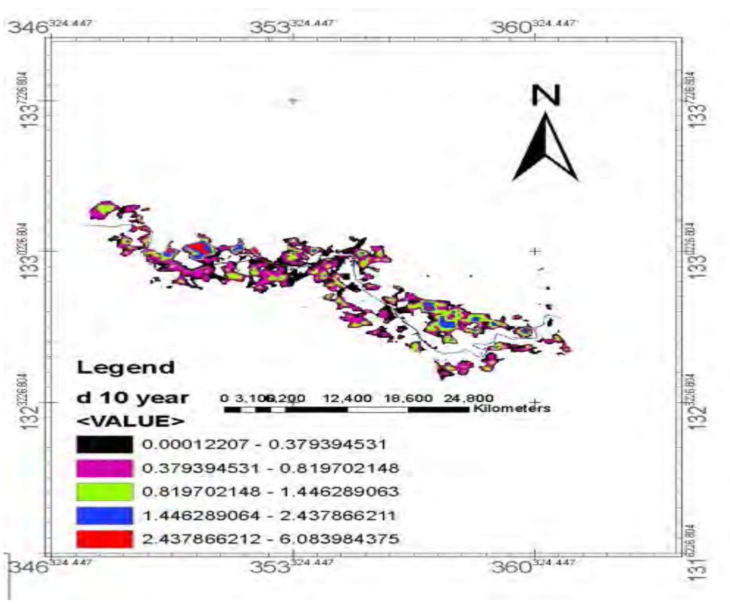

Fig D2**:** 10 year flood map

Appendix E: ENTRO flood result

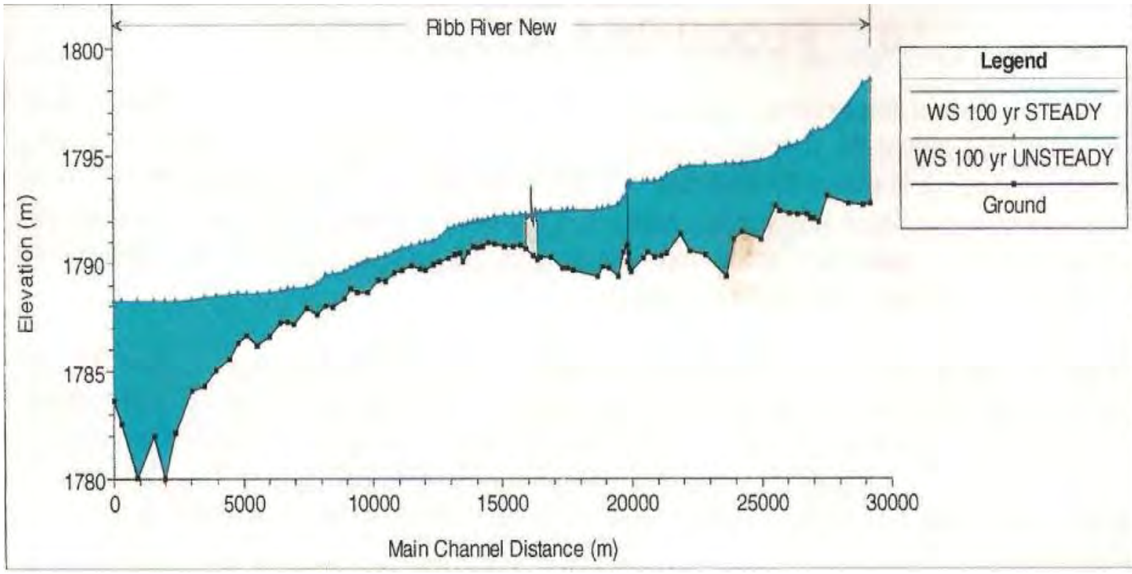

Fig E1: Water surface profile for 100 year

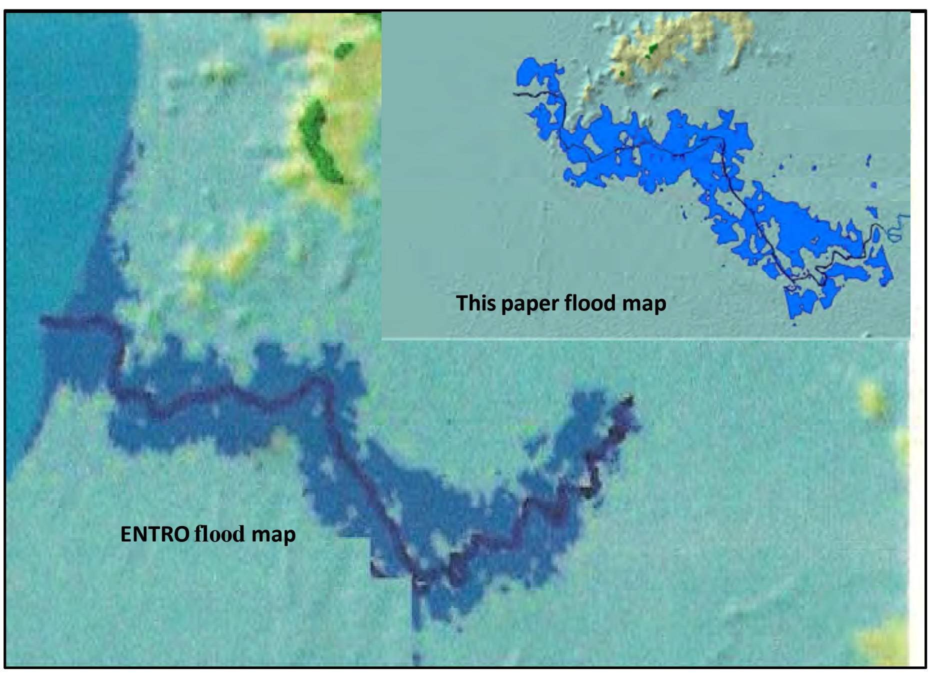

Fig E2: Flood map of ENTRO and this paper